University of Stavanger

Faculty of Science and Technology

MASTER'S THESIS

Study program/ Specialization: Offshore Technology/Marine and Subsea Technology	Spring semester, 2013 Open
Writer: Jacob Comuny Emesum	…… (Writer's signature)
Faculty supervisor: Prof. Arnfinn Nergaard External supervisor(s):Kjell Einar Ellingsen (Statoil ASA)	
Title of thesis: Full Scale Trawl Board Impact Testing In Water	
Credits (ECTS):	
Key words: Trawl board, Pipelines , Impact ,Energy, Subsea	Pages: 89 Stavanger, …06/06/2013…….. Date/year

Full Scale Trawl Board Impact Testing In Water

Master Thesis

Offshore Technology/Marine and Subsea Technology

Jacob Comuny Emesum

Spring 2013

ABSTRACT

During the last decades, the weights of trawl boards used in the North Sea, Norwegian Sea and the Barents Sea have increased significantly from barely a ton to a score of tons. In addition, the trawling speed has increased as well. These new faster and heavier trawl boards, in an event of impact with subsea structures, will result to tremendous loads on these structures. Impact with existing structures which were designed with recommendation from ISO 13628- part 1 may be devastating for the subsea structures as the new loads the structures will experience may be greater than its design loads.

Model trails performed in the late 80´s at a water depth of 100m, speed at 1,8 m/s and trawl board weight up to 1 900 kg resulted to an establishment of a design impact energy requirement of 13 kJ [9]. Statoil, in response to the increase in weight and velocity of trawl boards, raised their impact energy recommendation to 38 kJ.

This thesis aims at raising concerns on the level of conservatism in these values given that impact incidence that resulted to no damage at all on a subsea structure have been reported. It is worth mentioning that these structures were designed according to ISO 13628- part 1, but however the trawl board in this impact had a weight of 4 400 kg.
Statoil´s recommendation springs from impact test conducted in air and a theoretical study of the trawling situation for subsea structures from DNV report.
The following question arises: Is the Statoil´s recommended design impact energy of 38 kJ too conservative?

The goal of this work is to challenge this impact energy recommendation. This will be done by conducting a series of impact test on a copper pipe under the following configurations:

- An empty pipe will be impact tested in air.
- A closed pipe filled with water will be impact tested in air.
- A sealed water fill pipe will be impact tested in water.

The result from the following configurations will be analyzed and compared in order to determine the possible effect of damping (due to water in and out of the structure) on its response, laying ground work for a full scale test.

Acknowledgement

This thesis is dedicated to the memory of my beloved wife Bakhita Katume Nkofo, who's passing early this year has been very painful for our son and I. However, the support and encouragement she gave to me throughout my studies and even during her last days, gave me the strength required to complete this thesis on time.

This work would have been a fiasco without the love, and the very amazing patience my son Kristoffer Emesum demonstrated during this period. I appreciate his patience especially when I had to say to him too often `Not now, Kristoffer! I am working on my thesis´.

Special thanks to my supervisors Prof. Arnfinn Nergaard (University of Stavanger) and Kjell Einar Ellingsen (Statoil ASA-Stavanger) for their guidance, provision of literatures, equipment and comments which kept me on the right track.

I extend my gratitude to the mechanical engineering students working at the workshop in the University of Stavanger. They gave me a crash course in welding that was crucial in the building of the hammer used in this thesis.

I would like to thank Ahmad Yaaseen Amith (University of Stavanger) for the effort he put in making this work possible. At a very short notice, you thought me how to prepare and install strain gages and made available the various devices needed for the test.

And last but not the least, I wish to thank the following individuals whose encouragement contributed tremendously to the success of this thesis:

- Professor Ove Tobias Gudmestad
- Shaka and Adriana Nkofo
- The Yenwongfai family
- Dag H. Berg
- The Cameroonian associations in Norway
- Daniel Ebai Tambe and Enaka Enowntai
- Mercy Tyskerud and Esama Marceline
- Nyokabi Wanjiru Bækkelien and Noeline Goos

A very big thank you for all those whose names could not be mentioned here, I appreciate your efforts.

Contents

List of Figures

List of Tables

List of Symbols

W_s	Total elastic energy of the pipe
W_s	Strain energy per unit length
l ,L	Length of the pipeline
A	Cross-sectional area of pipeline
E	Young´s modulus of elasticity
ε	Strain
ε_{max}	Maximum strain
W_o	Total kinetic energy of impact
W_T	Total strain energy density
W_p	Plastic energy density
R	Mean outer radius of pipeline
r_o	Radius of deformed cross-section of pipeline
D	Outer diameter of pipeline
D_m	Maximum width of the deformed pipeline´s cross-section
T_r	Local permanent thickness of deformed cross-section
W_f	Maximum permanent transverse displacement
W_g	Permanent global displacement
W_l	Local displacement
E_{pl}	Energy absorbed by pipeline plastically
E_{gl}	Energy absorbed by pipeline globally
E_{mem}	Energy absorbed by pipeline´s shell membrane behaviour
Δ^{γ}	$W_l/2R$

$\Delta^{\gamma m}$	Dimensionless indentation
λ	Dimensionless kinetic energy
W^{γ}	W/2R
G	Mass of striker
H	Wall thickness of pipeline
σ_y	Uniaxial yield stress of the pipeline material
V_o	Initial impact velocity of striker
V	Velocity of trawl board
Es	Trawl boards' impact energy
R_{fs}	Reduction factor depending on the outer pipe diameter
m_t	Trawl board steel mass
C_h	Span height correction factor for effective pull-over velocity
m_a	Trawl board´s added mass
k_b	Lateral bending stiffness of the trawl board
α_U	Material strength factor
E_a	Impact energy associated with impact force
$f_{y,temp}$	Temperature derating value of the yield stress
f_y	(SMYS- $f_{y,temp}$) α_U
t	Steel wall thickness
E_{loc}	Kinetic energy absorbed by local deformation of the coating and pipe wall
C_b	Effective mass factor
σ_t	Tensile strength
ν	Poisson´s ratio
E_T	Calculated impact energy using Ellinas and Walker´s theory

$E_{T\text{-}DNV}$	Calculated impact energy using DNV-RP-F111

Abbreviations

SMYS	Specified Minimum Yield Strength
DNV	Det Norske Veritas

Chapter1 Introduction

1.1 Background

The coexistence of the petroleum and fishing industries as a matter of fact, has led to inevitable interactions between the equipment and structures in use by these sectors. It is well known that subsea structures are sites of attraction for various types of fishes and hence the regions around these structures turn to be great fishing grounds for fishermen. It is therefore obvious that fishing around these subsea structures will increase the likelihood of interaction between the fishing gears and the subsea structures such as pipelines, well heads, templates etc. a situation that may lead to the damage of both the fishing gear and the subsea structures.

In some areas of the Norwegian Continental Shelf, structures like pipelines are buried as a preventive method. However, for larger structures, burial is not a feasible option and hence there is a need to design them in such a way that they interact with these trawl gear, resulting to little or no damage for both equipment i.e. the subsea structure is overtrawlable.

In the Norwegian Continental Shelf, the Norwegian Petroleum Directorate set requirements for the design and installation of subsea structures and according to ISO 13628: Petroleum and gas industries- design and operation of subsea production systems part 1, subsea structures shall be designed for trawl board interactions i.e. impact, snagging and pull over.

Nowadays, the weights of the trawl board in use in the North sea, Norwegian sea and the Barents sea have increased significantly from the past 20 years: from 1500 kg in the early 80´s to 4 000 kg in 2005 [5] and possibly more than 6 000 kg in 2013.
Not only have the weights increased, the trawl velocities have also been increased up to 4 m/s. This increase in both the velocity and the weight will result to an increase in the impact force as well as the impact energies on the structures. It follows that the design loads and impact energy recommended by both the NORSOK U-001 and DNV-RP- F111 may no longer be relevant. Therefore there is a need for revised version of these recommendations.

In a move to accommodate these changes in trawl board properties, Statoil increases both the trawl board pullover and impact design loads; with the impact energy increased to 38 kJ from a previous 13 kJ. A recommendation that may be pretty much conservative given that mainly traditional Finite Element Analysis in air was performed with these new trawl board properties and a full scale test was not performed in water.

1.2 Project Scope

This thesis entails the following:

- An impact test is executed on three separate set of pipeline: empty pipes in air, water-filled pipes in air and water-filled pipes in water.
  Each set of pipelines will be tested with different loads so that a sensitivity study can be done on the effect of load variation.

- Measurements of the various geometric parameters on the deformed pipelines cross-sections and the use of these parameters as input data for recognized theoretical models. The outcome is the calculated values of plastic and global energies.

- Comparisons of the results obtained from all three groups. The aim is to bring out the differences in deformed geometry, energy absorbed by the pipeline for the various groups, etc.

- Computation of the impact energy absorbed by the pipelines using DNV-RP-F111 and compare these with values obtained using the theoretical models.

1.3 Project Organization

This project is organized as follows:

Chapter 2 This section describes the main fishing gear in use in the Norwegian and North seas. It also describes parts of these fishing gear, focusing on those parts that interact with subsea structures such as trawl boards.

Chapter 3 Here the various interaction scenarios between trawl boards and subsea structures are discussed, but emphasis is made on impact between these gear and submarine pipelines. Other interaction scenarios are simply introduced.

Chapter 4 This section deals with theoretical models developed for the deformation of pipelines due to impact. Two widely accepted theories are introduced. Given that these theories agree very well with experiments, they will be used further in this work.
The necessary parameters to be measured on the deformed cross-sections are defined.

Chapter 5 In this chapter, the DNV´s simplified method for the calculation of impact energy absorbed by a pipeline is summarized. This chapter also discusses and compares the design load requirements stated by NORSOK U-001 and the Statoil´s internal practice. Emphasis is laid on the difference between the trawl board impact design loads specified by both documents.

Chapter 6 The conducted test is described in details here. The design of the impact hammer is illustrated. The test procedure for each group, other devices used in the test as well as the data collection methods, is outlined.

Chapter 7 In this section, the results from each group of pipelines are presented and comparisons are made between the groups in terms of local indentation, local and global displacements, plastic and global energies etc. Calculated impact energy absorbed by pipelines using DNV is compared to that using one of the theoretical models.

Chapter 8 Conclusion and recommendation for further work is made in this section

Chapter 2 FISHING GEAR

There are numerous types of fishing gear being put into use by the commercial fishing industry worldwide. Some of these fishing gear are: Seine Nets, Trawls, Dredges, Hooks and Lines etc. Trawl gears are much in use by the commercial fishing industry on the Norwegian continental shelf. In this chapter, a brief description of numerous fishing gear, their design methodologies, names of vital parts and the breaking load for those important parts that interact with subsea structures. In order to grasp an extensive knowledge on how these operate, operational procedures will be covered and area of operations in the Norwegian and the Barents seas will be illustrated.

There following fishing gear are currently in use in most fishing areas in the world:

- Bottom trawl with heavy bobbins e.g. Otter trawl
- Pelagic or mid-water trawl
- Pair trawl
- Beam trawl
- Purse seine
- Seine netting
- Gill net
- Long line

In the North and Norwegian seas, it is worth noting that bottom otter trawl and beam trawl gears are commonly used.

2.1 Bottom Trawl Gear

These are widely used in the Norwegian waters. It consists of a net that is kept opened by either a door or a series of weights attached to it. The net is dragged on the sea floor often at a speed of 4 Knots (7km/h) [4], catching ground fishes and other species on its way. The trawl net may be drag on the seabed or mid water level, depending on the type of species that are targeted. There are two types of bottom trawl gear: the bottom Otter trawl gear and the bottom pair trawl rigging gears.

2.1.1 Bottom Otter Trawl

This gear is shaped like a bag and it is kept opened by otter boards. The otter boards move apart as they are pulled due to the hydrodynamic lift force acting on them. The trawl is towed along the sea bed to catch up fishes on the sea bed (figure 2-1)
The Otter trawl gear consists of a large net, kept opened by trawl boards/doors. This trawling takes place in a water depth up to and above 400m.

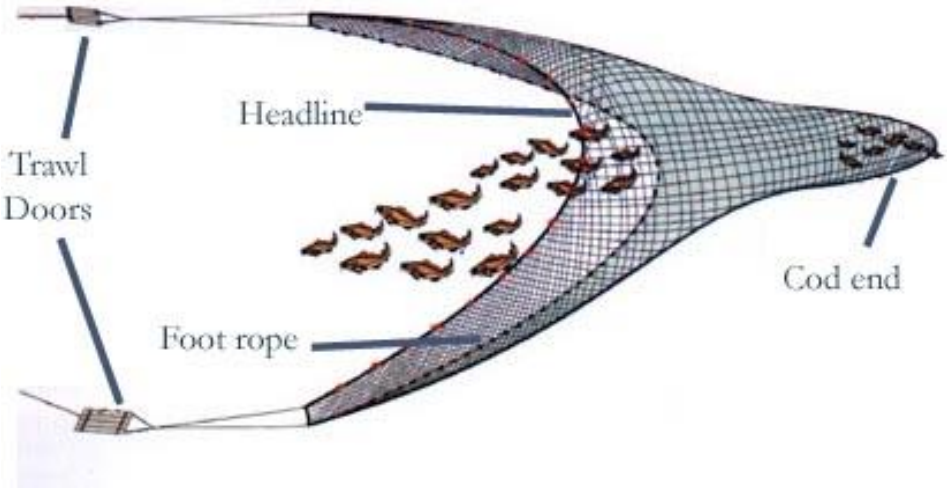

Figure 2-1 Illustration of the main part of an Otter trawl (stripersonline.com)

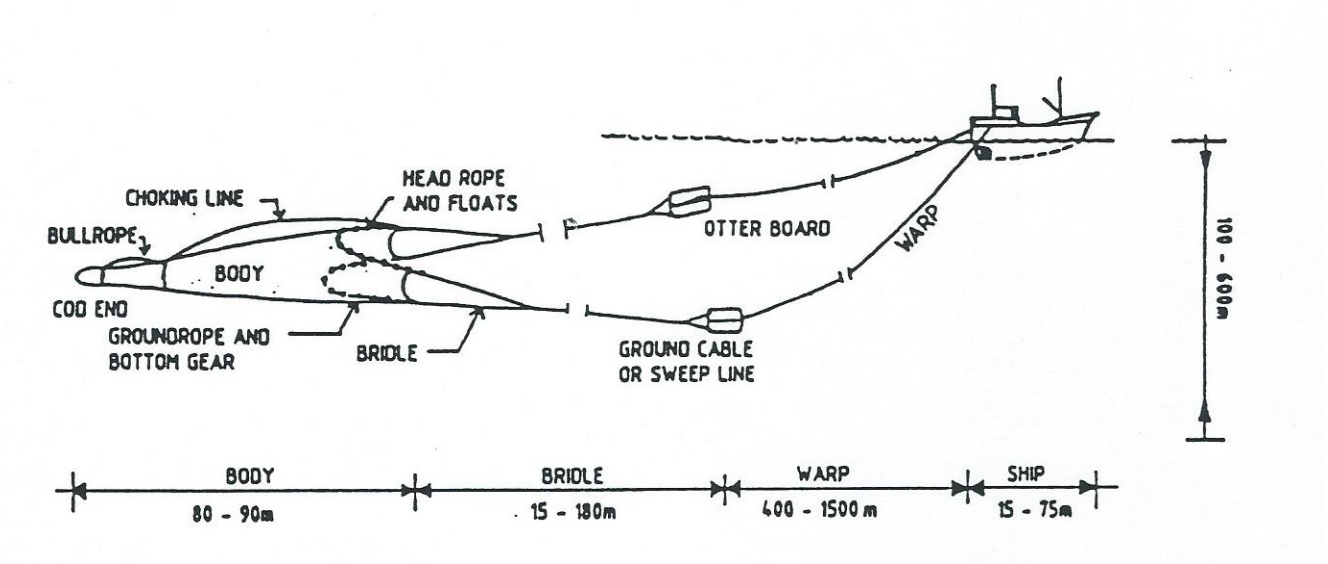

Figure 2-2 Detailed illustration of an Otter trawl with standard dimensions [2]

2.1.1.1 Ground Rope

Depending on the water depth, the ground rope will be made up of different materials such that it has enough weight to scrub the sea bottom while it is being pulled along. In shallow waters e.g. Coastal waters, light ground rope are used while in deep waters, heavy ground rope i.e. steel bobbins are used. The heavy ground rope is necessary for shrimp catch as suggested by Deshpande and George (1965).

Some of the ground rope configurations are described in the figure below:

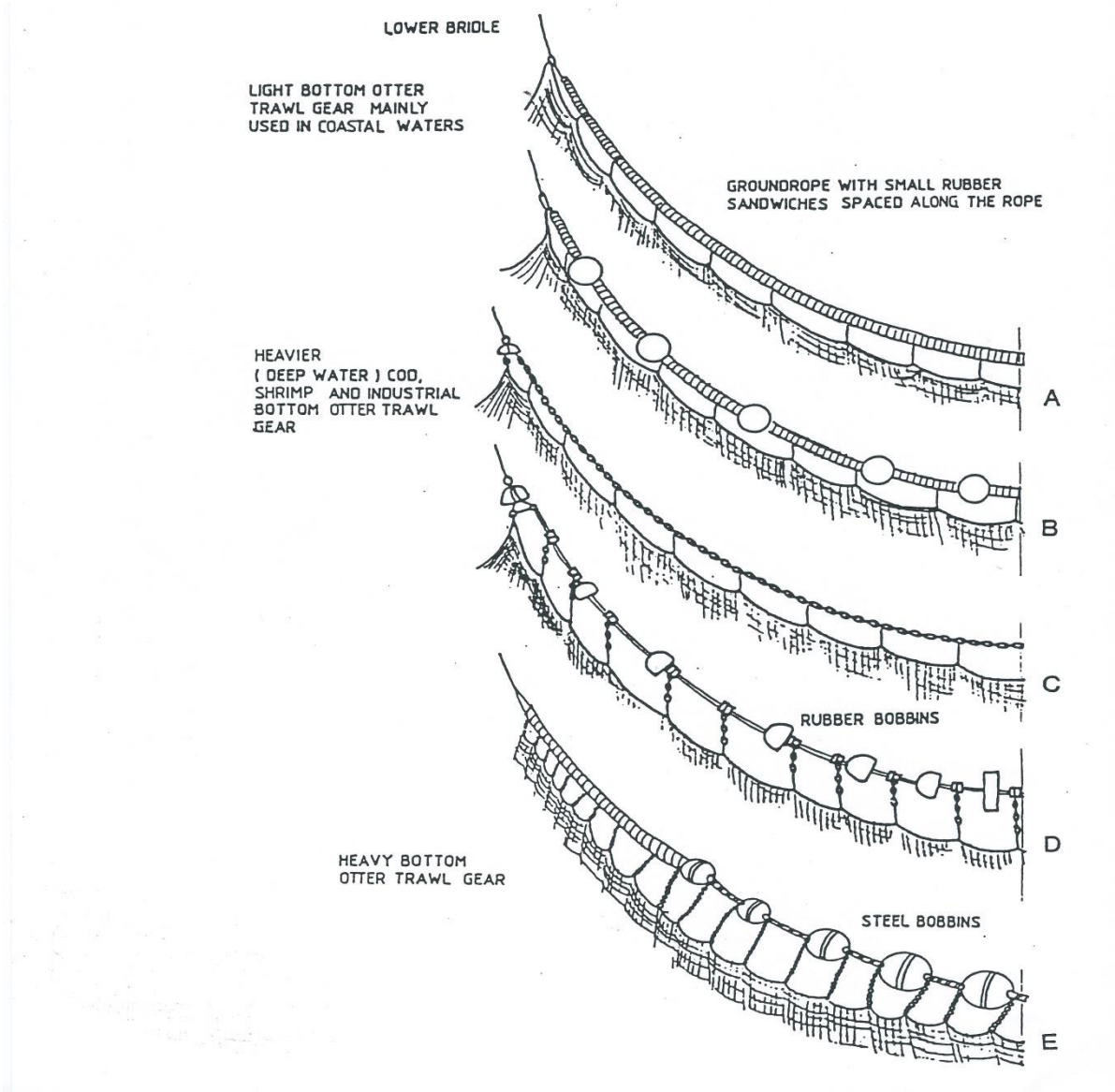

Figure 2-3 Different types of ground rope for Otter trawl [2]

2.1.1.2 Otter Boards

Otter trawl doors/boards are made of steel or wood and are designed in such a way that they flow through water at a certain inclination. This inclination, combined with hydrodynamic lift force acting on it, cause a spread of the doors from each other resulting to the opening of the net in a horizontal direction. Trawl warps are used to attach the boards to the ship.

The weight and shape of the Otter trawl have so much to say about its hydrodynamic efficiency. For this reason, many different types of board designs are used in the fishing industry as manufacturers attempt to improve on the gear´s efficiency.
There are principally three main different shapes of Otter board in use in the Norwegian trawl fishing industry:

Figure 2-4 Illustration of a typical standard rectangular Otter door [6]

The standard rectangular board are easily constructed and maintained. The earliest known boards were of this type. The cost of constructing these boards is quite low as the board is mainly made up of wood.

Figure 2-5 An illustration of a V-shaped Otter door [6]

The V-type (vee) door is the most commonly used otter board in the North Sea despite its low efficiency. However, it is relatively cheap to construct and operate. Altering the shape of the plate can increase the water flow around the board considerably, improving on its performance. This is typical of a cambered V otter board

Figure 2-6 An illustration of a typical oval shaped Otter door[6]

The Oval doors are quite extensively used by deep sea fleet. They are suitable for fishing over rough sea beds.

Otter doors are classified according to their dimensions and weights. The table below shows some principal dimensions in the late 70s:

Type	In mm		Gross area m^2	Weight of one door(kg)	
	Length	Height		In air	Submerged
1	2050	1210	2,00	560	330
2	2255	1330	2,35	640	380
3	2360	1390	2,75	685	410
4	2750	1580	3,50	930	560
5	3120	1780	4,45	1180	670
6	3120	1780	4,45	1280	760
7	3450	1970	5,27	1450	850
8	3750	2150	6,30	1765	1040
9	4000	2300	7,40	2050	1200

Table 1-1 Classification of Otter doors based on their dimensions and weights [2]

These values are based on survey conducted in the late 70s. However, the weights and dimensions of Otter doors have changed enormously since the 70s. In 2007, the weights of Otter doors have increased up to 6000 kg [5] and perhaps 10000 kg in 2013.

2.1.2 Bottom Pair Trawls Rigging and Double Bottom Trawl Rigging

These gear are similar to the above mentioned gear but differ in the fact that:

- There are no Otter doors. Instead, clump weights or a length of heavy wires are used to keep the gear on the sea bed. The lack of doors result to extremely small hydrodynamic lift force and therefore the need for two separate vessels, pulling the warps away thereby keeping the net open.(figure 2.7)

- There are Otter doors (two),however two nets are connected together in such a way that they have a common weep line attached to a clump weight .A single vessel is requited to tow the net as the doors keep the nets open.(figure 2.8)

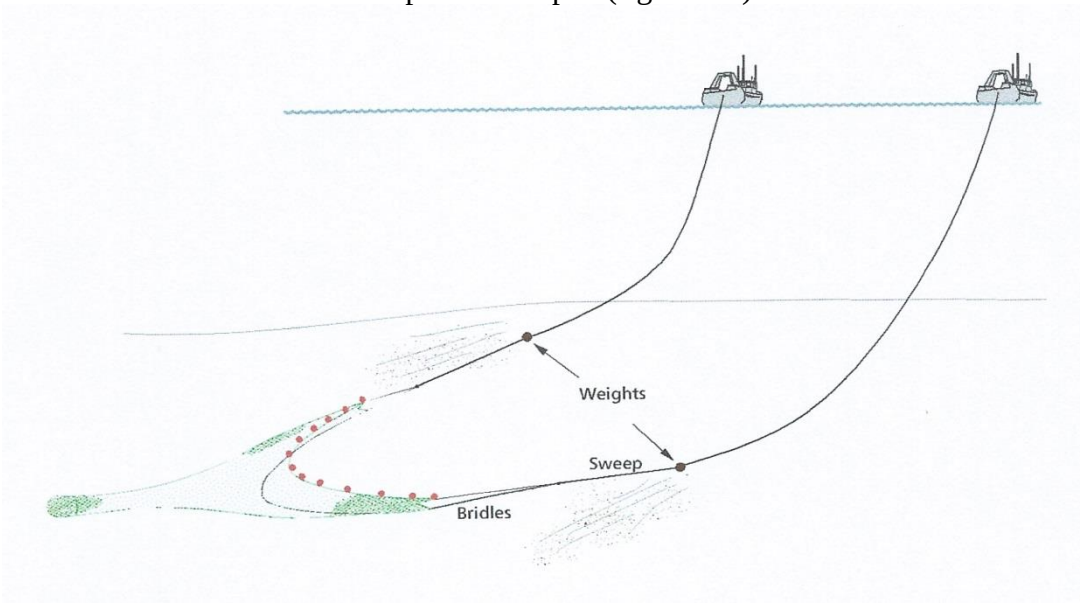

Figure 2-7 Illustration of bottom pair trawl rigging technique [6]

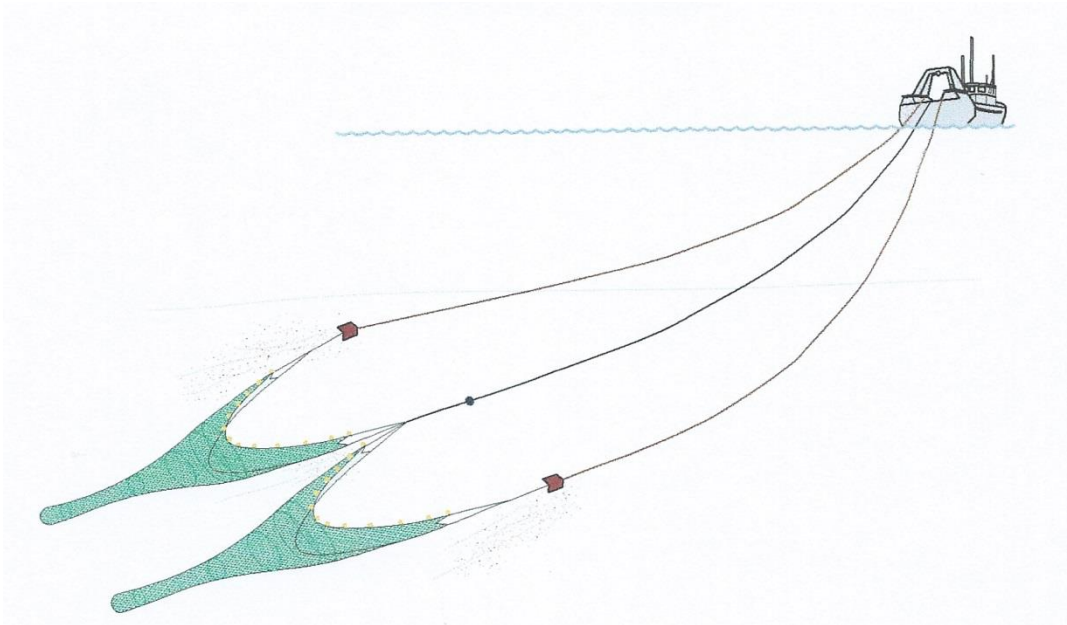

Figure 2-8 Illustration of double bottom trawl rigging technique [6]

2.1.2.1 Bottom Trawl Fishing Area

Bottom trawl are widely in use in the North Sea, the Norwegian continental shelf, the Barents Sea and the area off the Svalbard islands. Demersal species such as Norway pout, prawn, redfish, cod etc. are the principal targets for this fishing method. The map below shows the area of frequent bottom trawl activities (gray area):

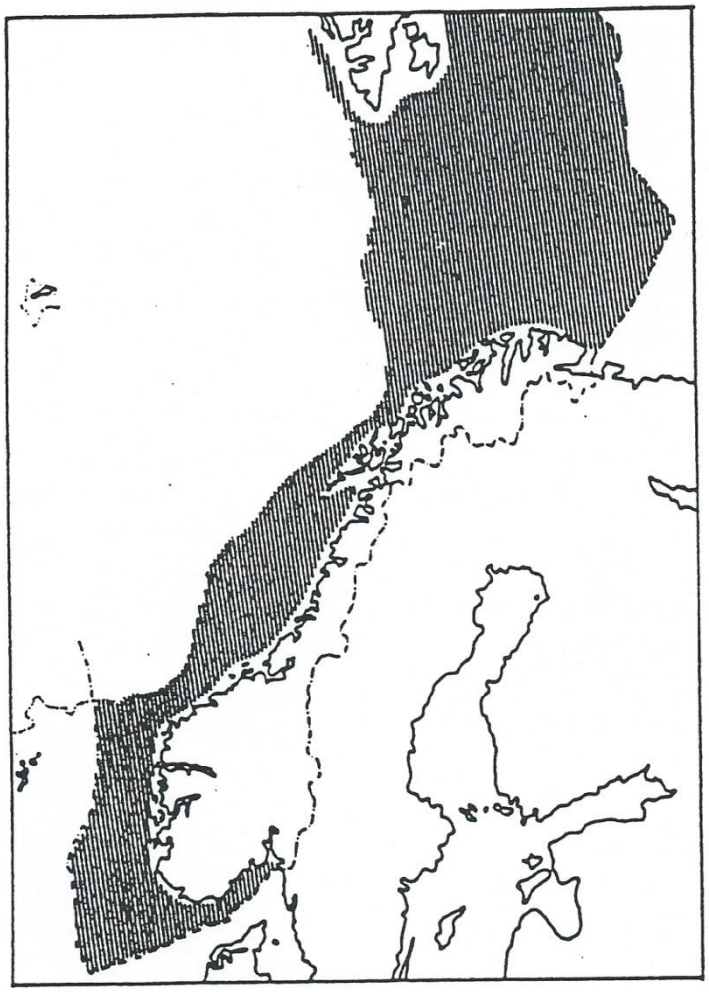

Figure 2-9 Area of operation for the bottom trawl [2]

2.1 Beam Trawling

A standard beam trawl consists of a steel beam having trawl shoe (head) in each of its ends. A trawl net is placed with its upper part attached to the beam and the lower part, to the ground rope. Two bridles are linked to each of the trawl shoes, the steel warp and also to the middle of the beam; this ensures the stability of the trawl gear.

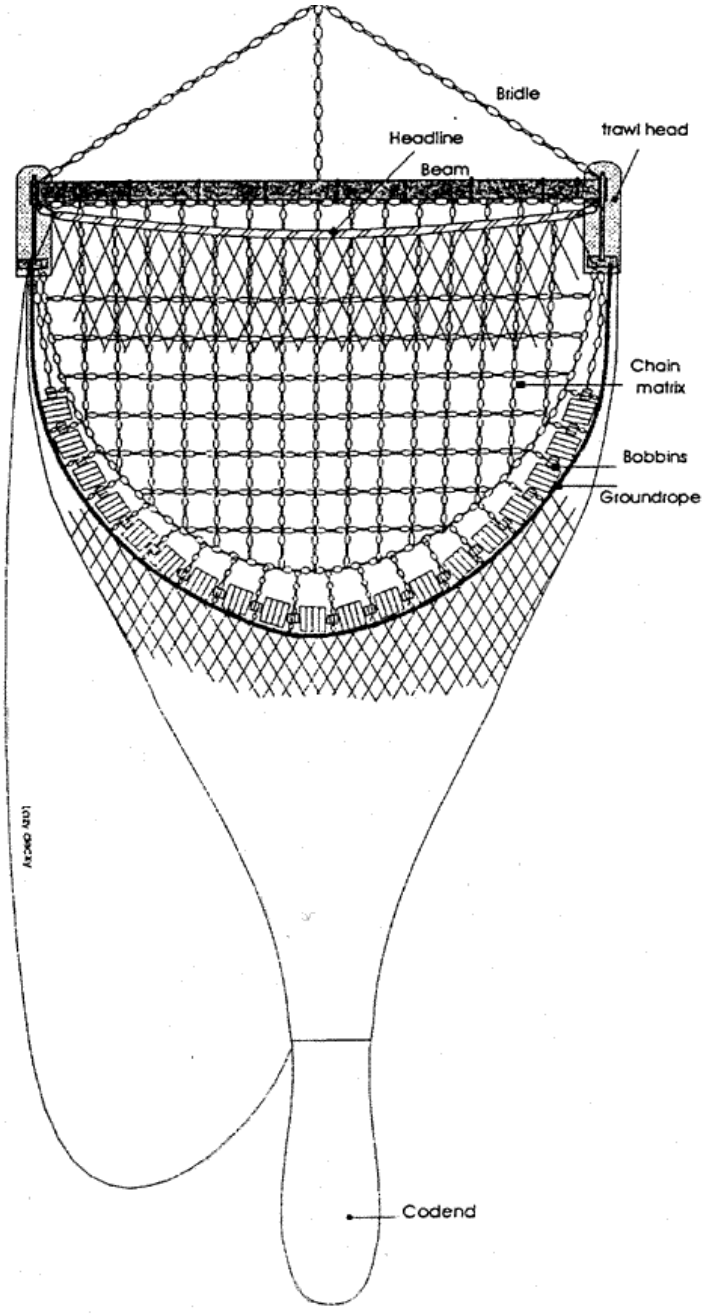

Figure 2-10 A conventional beam trawl [7]

Due to growing concern about the devastating effect of the beam trawl on the community of benthic animals, a new type of beam trawl was introduced .In this version, the chain matrix has been replaced by cables with electrodes, producing electricity that startles the fish [8].

Chapter 3 Trawl Gears Interaction Scenarios with Subsea Structures

The interaction scenarios between a trawl gear and a subsea structure is basically divided into two different phases: Impact and Pull-over. However, interactions such as hooking, sweep lines, net friction etc. may be considered where necessary.

3.1 Impact

This is the initial stage where the trawl gear hits the subsea structure. This interaction usually last for a hundredth of a second .In case of a submarine pipeline, it is mainly restricted to the coating and the pipes shell. For a submarine pipeline laid on the sea bed, the energy from impact is transferred to the pipe, it´s coating and to the soil. All of these offer a certain level of resistance to the impact force. The pipe´s resistance to the impact load may lead to local and in some cases, global deformation and dent in the pipe wall as well.

There are basically two impact scenarios between a trawl gear and a subsea structure:

- Trawl gear direction normal to subsea structure

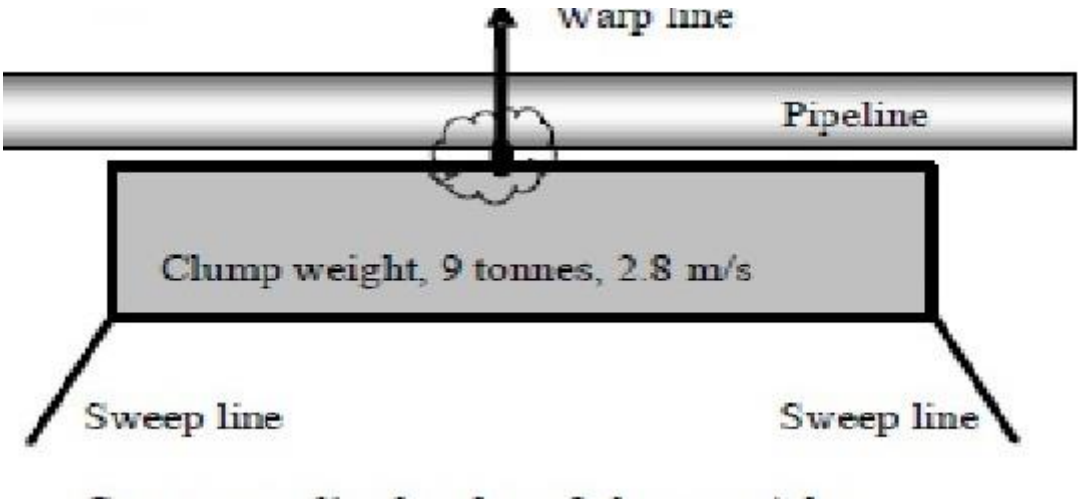

Figure 3-1 Iillustration of a trawl gear impact normally to a submarine pipeline [5]

In this type of impact, there is no reduction in the impact energy as the trawl gear does not rotate i.e. it hits the structure head on. If the gear comes to rest after impact, then its initial kinetic energy would be transferred entirely to the structure. In most situations, the gear does not come to rest after impact. It is rebounded with some of its initial kinetic energy.

- Trawl gear travels at an inclined angle to the pipeline

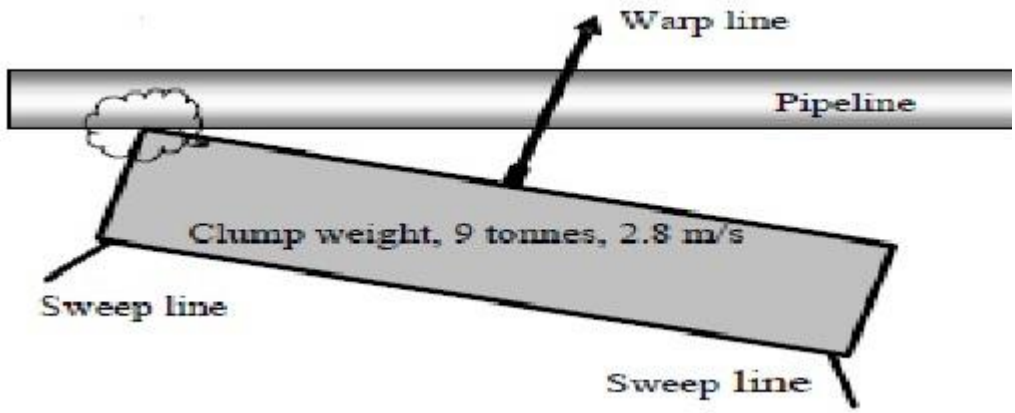

Figure 3-2 Illustration of impact between trawl gear and subsea structure at an inclined angle [5]

Due to the angle of incline, only a fraction of the gear´s initial kinetic energy will be transferred to the structure

3.1.1 Impact Energy

When a pipe is subjected to impact normal to its length, the impact energy distributes itself in the pipe in a complex manner. However, the energy transformation from one form to another is rather simple to understand. The energy transferred can be divided into three stages:

- Before impact, the energy of the system comprises of only kinetic energy of the hammer.

- During impact, part of this translational kinetic energy of the hammer is transformed into strain energy in both the pipe and the hammer whereas some part is transformed into vibrational energy in the hammer, pipe and even the support on which the pipe is placed.
  If the support is perfectly rigid, there will be no vibrational or strain energy transferred to the support. However, it is impossible to make a support perfectly rigid.
  The stress wave generated by the impact propagates through the material, dissipating a negligible trace of the energy in the form of heat.

- A rebound of the hammer may occur. This is due to a fraction of the strain and vibrational energy in the system been converted to kinetic energy of the hammer.

3.1.1.1 Calculation of Strain Energy Due To Impact

3.1.1.1.1 Elastic Strain Energy

In theory, the amount of strain energy in the pipe prior during impact determines the size of the dent and the bending in the pipe. The determination of the amount kinetic energy converted to strain energy is very important.

Consider a pipe under the following state of strain:

- Uniform strain at any cross-section of the pipe.
- Variable strain at different cross-sections of the pipe.

The total strain energy of the pipe may be determined as follows:

$$W_s = \int_0^l w_s \, dl \qquad (1)$$

Where W_s = Total elastic (linear) strain energy of the pipe
w_s = Strain per unit length of the pipe
l = Length of the pipe

At a given section, the elastic strain energy per unit length is given by the relation

$$w_s = \frac{AE\varepsilon^2}{2} \qquad (2)$$

Where A = cross-sectional area of the pipe
E = Young´s modulus of the pipe´s material
ε = strain

It follows from equation (1) and (2) above that the total elastic strain energy of the pipe is given by:

$$W_s = \frac{AE}{2} \int_0^l \varepsilon^2 \, dl \qquad (3)$$

The strain energy in the pipe at any time can be expressed as a fraction of the total kinetic energy of impact W_o.

$$\frac{W_s}{W_o} = \frac{AE}{2} \int_0^l \frac{\varepsilon^2}{W_o} dl \qquad (4)$$

The following conclusion can be made based on experiment conducted Richard J. Charles [11]:

- The ratio $\frac{\varepsilon_{max}}{\sqrt{W_o}}$ is constant for impacts with any hammer
- The ratio $\frac{\varepsilon_{max}^2}{W_o}$ is a measure of the fraction of kinetic energy of impact which is transformed to strain energy in the gaged section of the pipe.

3.1.1.1.2 Plastic Strain Energy

A metal may yield under impact such that it deforms and do not return to its initial state after impact and or unloading.

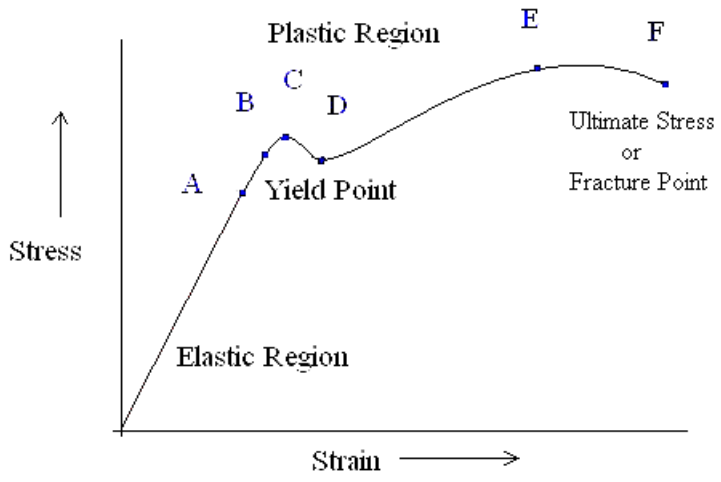

Figure 3-3 A typical stress-strain curve [12]

The point B is called the yield point. This is the point after which the material undergoes inelastic or permanent deformation.
There are many criteria used to predict the initiation of yielding: Rankine´s criterion, St. Venant's criterion, Tresca criterion etc.
When a material is loaded until the yield point is exceeded i.e. in the plastic region, the total strain energy density in the system (W_T) consists of two parts: Elastic strain energy (W_s) and Plastic s energy (W_p) densities.

$$W_T = W_s + W_p \qquad (5)$$

3.2 Pull-Over

Pull over is the secondary phase. The gear is pulled over the structure as the vessel continues forward. The structure experiences huge vertical and horizontal forces, which can last up to a dozen seconds. The duration of the pull over will very much depends on: the velocity of the trawl gear, the stiffness of the warp line etc. As oppose to impact that mostly lead to a local response, pull over results to a global response from the structure.

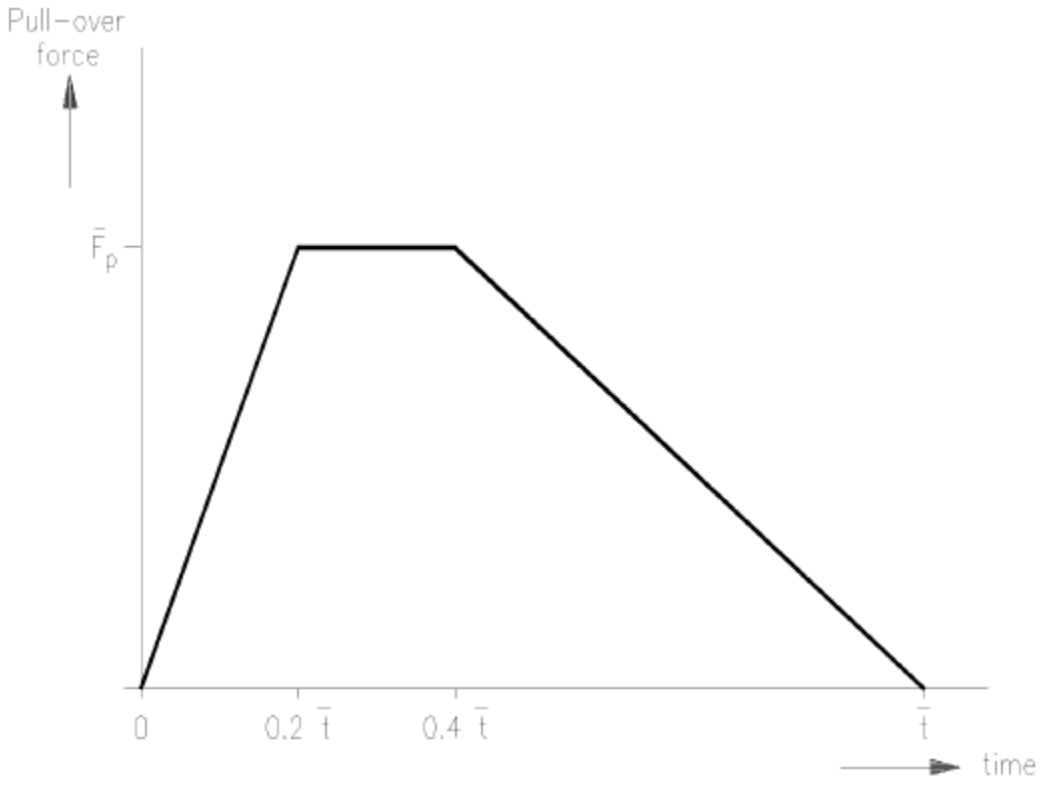

Figure 3-4 Trawl board pull-over force-time history for rectangular and V boards [21]

3.3 Hooking

Hooking is a rare interaction between trawl gear and pipeline. It generally involves the trawl gear been wedged under the pipeline.The result of such interaction is that the pipeline might be lifted and experience large vertical load as the trawler tries to free the gear.
The pipeline may be deflected laterally during hooking. Yielding and local buckling may be initiated during hooking as well.

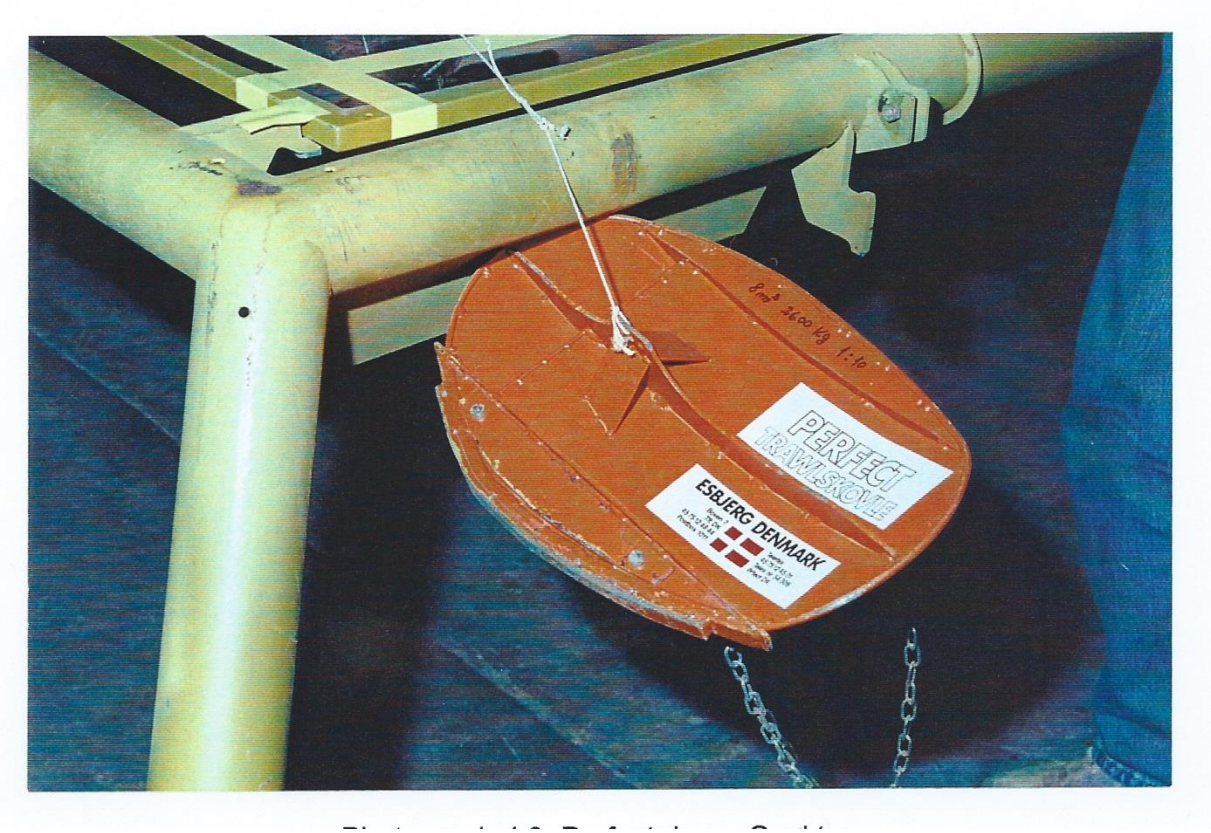

Figure 3-5 Hooking scenarion between a tubular structure and an oval door [22]

Chapter 4 Theory on Deformation of Pipelines Due to Impact

4.1 General

The response of a pipeline clamped at both ends and struck transversely on the span, consists of both local indentations and a global beam-like behavior. If the impact load is sufficiently large enough, deformations (failure modes) of the pipeline may be visible. The type of failure modes will then depend on the impact face of the striker. The striker may have different types of shapes e.g. conical, spherical, wedge, octagonal, blunt etc. For example, Jones et al [16] demonstrated that a wedge shaped striker do not perforate a pipeline on impact, but it however causes a localized crack which may result to a slow leakage or a more global failure at the supports with the possibility of the pipe´s content been released.

Looking at the picture of a deformed pipeline (see fig below), it is obvious that the total displacement is made up of a local (change in cross section) and a global (beam-like) displacements.

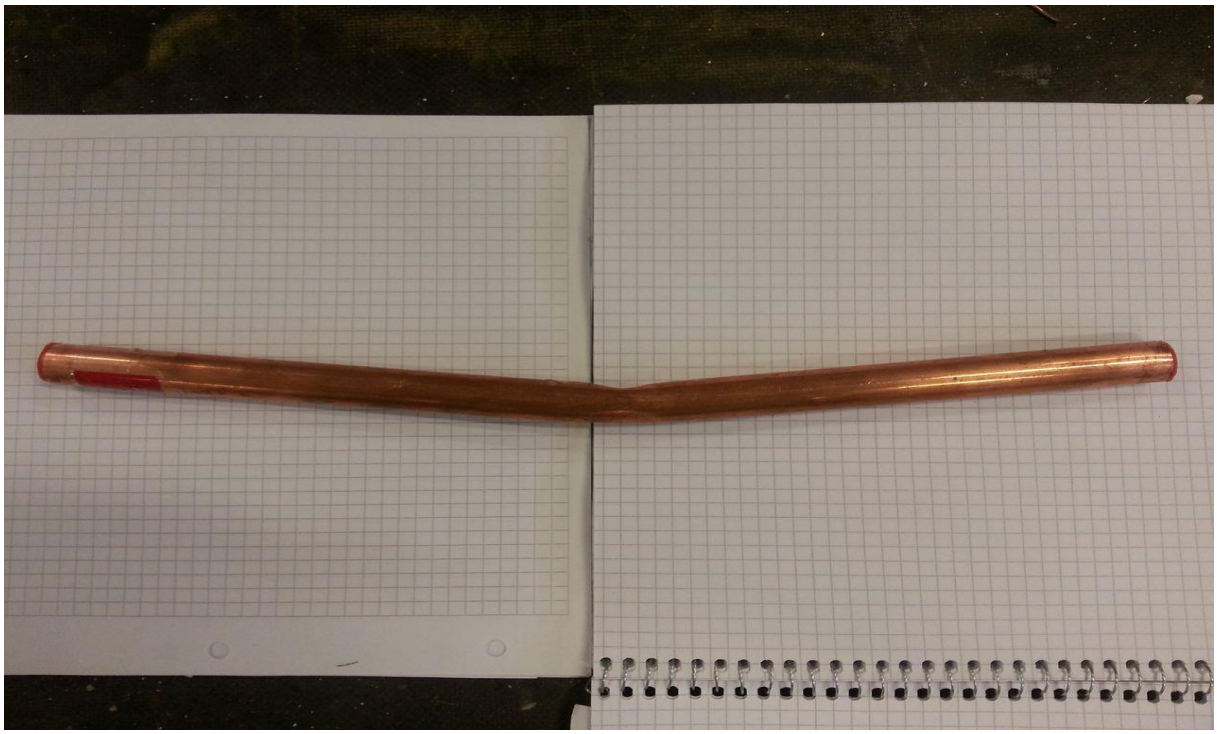

Figure 4-1 A deformed pipeline clamped at both ends (after impact)

The pipeline before impact has a mean radius R. The deformed geometry can be idealized as shown in the figure below, using the following assumptions:

- After impact the pipeline´s cross section under the indenter is deformed into a circular profile with radius r_o and closed with a chord.
- The center of the un-deformed cross section, generally used to define the global displacements coincides with the equal area axis of the deformed section.

Figure 4-2 A section through a deformed pipe showing the deformed geometry

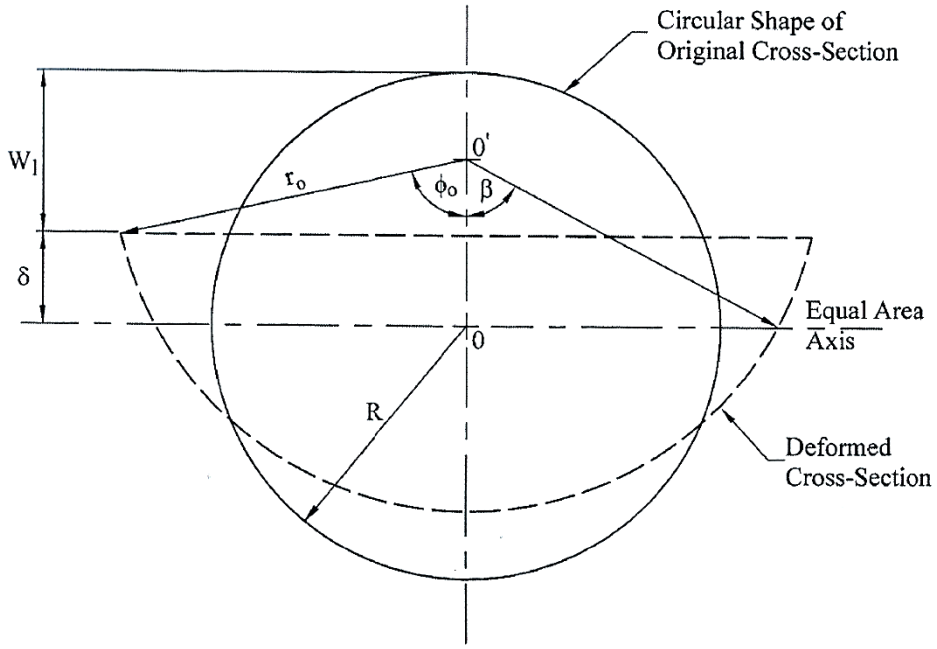

Figure 4-3 Deformed and un-deformed cross-sections of a pipeline in the impact plane [13]

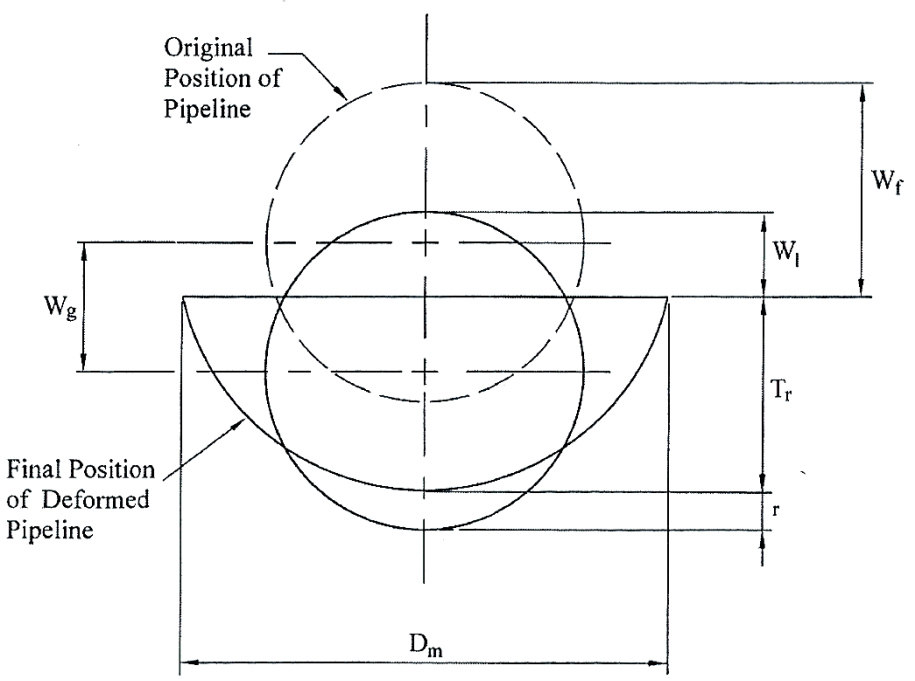

Figure 4-4 Definition of local indentation,global displacement and total displacement for the idealised deformed cross-section [13]

4.2 Determination of the Local and Global Displacements.

The local and global displacements can be obtained from these three measurements:

- The overall permanent displacement (W_f)
- The local permanent thickness of the deformed cross-section (T_f)
- The maximum with of the deformed cross section (D_m)

The radius of the deformed cross-section can be computed from the relation shown below [17]:

$$r_o = \frac{T_r}{2}\left[1 + \left(\frac{D_m}{2T_r}\right)^2\right] \qquad (6)$$

Where T_r is the residual thickness across the deformed profile at the impact location. Both T_r and D_m can be measured after the impact test.

The angles β and ϕ_o are given by

$$\beta = \pi \frac{R}{2r_o} \tag{7}$$

and

$$\cos\phi_o = 1 - \frac{T_r}{r_o} \tag{8}$$

The local displacement (W_l) is estimated as

$$W_l = R - \delta \tag{9}$$

Where

$$\delta = r_o(\cos\beta - \cos\phi_o) \tag{10}$$

The permanent global displacement is then given by

$$W_g = W_f - W_l \tag{11}$$

4.3 Theories on the Local and Global Plastic Energies Absorbed During Impact

Much research has been done on pipelines under impact loading using numerous types of strikers. Although it is very complex to quantize the amount of impact energy transferred to plastic energy in the material, theories on plastic energies absorbed during impact has been proposed, tested and accepted, some of which will be summarized below:

4.3.1 Theory of Ellinas and Walker

Consider a fully clamped rigid, perfectly plastic pipeline struck at the mid span (L_1=L) by a mass G with velocity V_o as shown in the figure below.

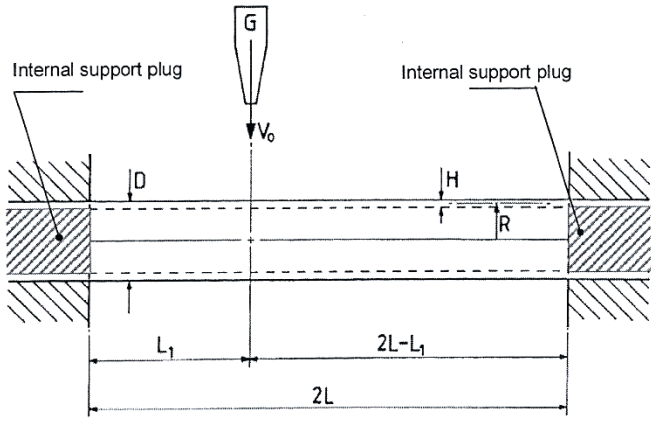

Figure 4-5 A fully clamped pipeline struck by a mass G travelling at a speed V_o [13]

The energy absorbed by the pipeline plastically during the local indentation phase is given by

$$E_{pl} = \frac{KRH\sigma_y}{3}\left(\Delta^{\gamma}\right)^{\frac{3}{2}} \qquad (12)$$

$$0 \le \Delta^{\gamma} \le \Delta^{\gamma_m}$$

Where

$$\Delta^{\gamma} = \frac{W_1}{2R}$$

And K=150.

The dimensionless indentation at the start of global deformations Δ^{γ_m} is given by

$$\Delta^{\gamma_m} = \left[32R^2\frac{(1+\cos\beta-\beta)}{KLH}\right]^2 \qquad (13)$$

With

$$\beta = 1 + \left(2\cdot\frac{R}{H}\right)\left[4\frac{\Delta^{\gamma_m}}{3} - \left[\left(4\frac{\Delta^{\gamma_m}}{3}\right)^2 + \left(\frac{H}{2R}\right)^2\right]^{\frac{1}{2}}\right]\Delta^{\gamma_m} \qquad (14)$$

In case of only local deformation i.e. insufficient kinetic energy to start global deformation, then

$$\lambda = \frac{KL\left[\left(\Delta^{\gamma}\right)^{\frac{3}{2}}\right]}{48R} \qquad (15)$$

Where
λ = dimensionless initial kinetic energy.

If the initial kinetic energy is sufficient enough to start a global deformation, then the following hold:

$$\Delta^{\gamma} = \Delta^{\gamma m} \qquad \text{And} \qquad W^{\gamma} > 0$$

The global energy absorbed is then given by:

$$E_{gl} = 16HR^{3}\sigma_{y}\left(1 + \cos\beta - \beta\right)\frac{W^{\gamma}}{L} \qquad (16)$$

4.3.2 Theory of Oliveira, Wierzbicki and Abramowicz

Base on the setup in figure 4.4, Oliveira et al [15] in their theoretical analysis worked out that the local denting behavior absorbs the external energy

$$E_{l} = 8\pi^{\frac{1}{2}}\sigma_{y}\frac{\left(HW_{l}\right)^{\frac{3}{2}}}{3} \qquad (17)$$

This is valid up to

$$\Delta^{\gamma m} = 2\left[k - \left(k^{2} - 1\right)^{\frac{1}{2}}\right] \qquad (18)$$

Where

$$k = 1 + \pi\frac{H\left(\frac{L}{R}\right)^{2}}{8R} \qquad (19)$$

The local behavior is assumed to cease when the global deformation starts. This happens when

$$\Delta^{\gamma} = \Delta^{\gamma_m}$$

The global energy absorbed plastically is given by

$$E_{gl} = \left(16\sigma_y R^3 \frac{H}{L}\right)\left[\left(\frac{8}{\pi^2}\right)\left(1-\Delta^{\gamma_m}\right)\left(2-\Delta^{\gamma_m}\right)\sin\left[\pi^2\frac{W^{\gamma}}{8\left(1-\Delta^{\gamma_m}\right)}\right]+\pi^2\frac{\left(W^{\gamma}\right)^3}{12\left(1-\Delta^{\gamma_m}\right)}\right] \qquad (20)$$

For larger global deformation than W^{γ_m} where

$$W^{\gamma_m} = 4\frac{\left(1-\Delta^{\gamma_m}\right)}{\pi} \qquad (21)$$

Some of the impact energy can be absorbed by membrane behavior of the pipeline shell. In this case, the global deformation W^{γ} is larger than W^{γ_m} i.e.

$$W^{\gamma} > W^{\gamma_m}$$

This energy is can be calculated from:

$$E_{mem} = \left(8\pi\,\sigma_y R^3 \frac{H}{L}\right)\left[\left(W^{\gamma}\right)^2 - \left(W^{\gamma_m}\right)^2\right] \qquad (22)$$

The total energy absorbed by the pipeline plastically will therefore be

$$W_p = E_{pl} + E_{gl} + E_{mem} \qquad (23)$$

Chapter 5 State of the Art

5.1 DNV

The DNV-RP-F111 recommended practice is widely used for the design of subsea pipelines in the oil and gas industry. The version dated 2010, proposed simple and conservative method to calculate the energy absorbed by the pipe locally based on the following assumptions [5]:

- The pipe deforms locally by indentation.
- All the impact energy is absorbed through indentation.

5.1.1 Impact with Trawl Board

In case of impact of a trawl board with a pipeline, the trawl board´s impact energy is given by:

$$Es = R_{fs} \cdot \frac{1}{2} \cdot m_t \cdot \left(C_h \cdot V\right)^2 \qquad (24)$$

Where

m_t = the trawl board steel mass.

R_{fs} = reduction factor depending on the outer pipe diameter (see figure 5-1 below).

C_h = span height correction factor for effective pull-over velocity (see fig 5-2 below).

V = velocity of the trawl board.

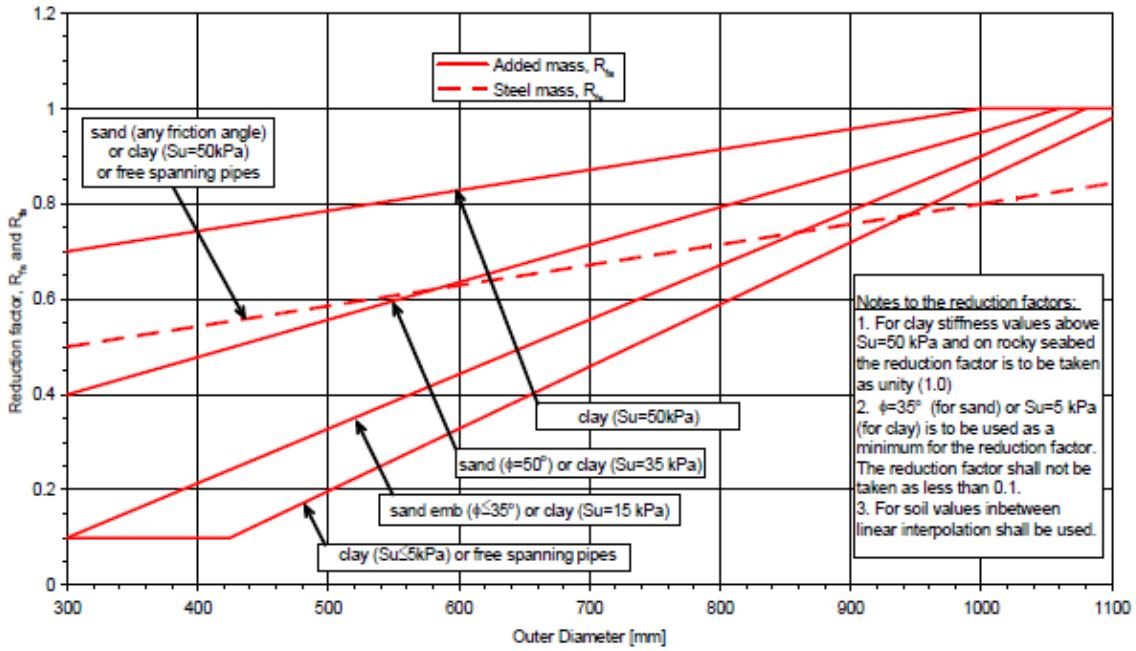

Figure 5-1 Reduction factors for concrete coated and bare pipes [5]

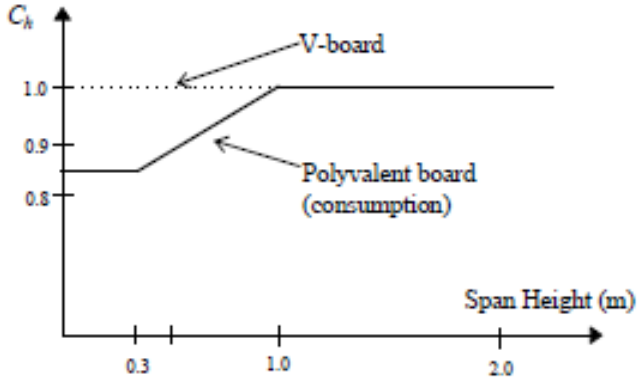

Figure 5-2 C_h coefficient for effect of span height on impact velocity [5]

As the trawl board moves in water, the hydrodynamic added mass of the trawl board contributes to the impact force. The associated impact force due to hydrodynamic added mass is given by:

$$F_b = C_h \cdot V \cdot \left(m_a \cdot k_b\right)^{\frac{1}{2}} \qquad (25)$$

Where

m_a = the trawl board´s added mass

k_b = the lateral bending stiffness of the board

The energy associated by this impact force is given by:

$$Ea = R_{fs} \cdot \frac{2 \cdot \left(F_b\right)^3}{75 \cdot \left(f_y\right)^2 \cdot t^3} \leq \frac{1}{2} \cdot m_a \cdot \left(C_h \cdot V\right)^2 \qquad (26)$$

Where

f_y = (SMYS – $f_{y,\,temp}$)α_U

$f_{y,\,temp}$ = the temperature derating value of the yield stress.

α_U = the material strength factor.

t = the steel wall thickness.

The kinetic energy absorbed by local deformation of the coating and the pipe wall is then:

$$E_{loc} = \text{Max (Es, Ea)}$$

5.1.2 Impact with Beam Trawl

The impact energy absorbed by the pipe and its coating in the case of a beam trawl is given by:

$$Eloc = R_{fs} \cdot \frac{1}{2} \cdot C_b \cdot \left(m_t + m_a\right) \cdot V^2 \qquad (27)$$

Where

C_b = A factor taking into account the effective mass and may conservatively be set equal to 0.5 if a more precise estimate is not available

m_t = The steel mass of the beam trawl with shoes inclusive

m_a = The hydrodynamic added mass including the mass of water entrapped in the beam.

5.1.3 Impact with clump weights

In the case of a clump weight, the total absorbed energy can be calculated from:

$$Eloc = R_{fs} \cdot \frac{1}{2} \cdot \left(m_t + m_a\right) \cdot V^2 \qquad (28)$$

Where

m_t = The dry steel weight of the clump weight

m_a = Hydrodynamic added mass of water entrapped in the sections.

The hydrodynamic added mass m_a can be calculated as follows:

- The mass of water displaced multiplied by 2.29. This is valid for impact closer to the sea bed.
- The mass of water displaced multiplied by 0.8 in case of limited length.

5.2 NORSOK U-001versus Statoil's Internal Practice

The design of subsea structures is mainly governed by ISO 13628-1, annex F (NORSOK U-001) requirements, especially for trawl loads. Model trails done in the late 80´s at water depth of 100m with a trawl board mass up to 1900 kg at a speed of 1.8 m/s, resulted to the design loads requirements shown in the table below:

Design load type	**Design load figure**		
Trawl net friction	2x200 kN	0^o to 20^o horizontal	ULS
Trawl board over-pull	300 kN	0^o to 20^o horizontal	ULS
Trawl board impact	13 kJ		ULS
Trawl board snag	600 kN	0^o to 20^o horizontal	PLS (if not overtrawlable/snag free)
Trawl ground rope snag	1000 kN	0^o to 20^o horizontal	PLS (if not overtrawlable/snag free)
Trawl board snag on sea line	600 kN		PLS (if not overtrawlable/snag free)

Table 5-1 Design load requirements for trawl gear -pipeline interactions [20]

The weights of trawl gear have increased tremendously since the 80´s. These increase, have called for concern on the design load requirements specified by ISO 13628-1. As a matter of fact, it is logical to step up the design load for pull-over and trawl board impact.

Statoil in its internal documents (TR1230) presented the following design loads and conditions:

Design load type	**Fixed generic trawl loads**		
	Design loads	Load condition	Direction
Trawl net friction	2x200 kN	ULS or ALS 1)	0^o to 20^o horizontal
Trawl board and equipment pull-over	450 kN 2) 3)	ULS or ALS 1)	0^o to 20^o horizontal
Trawl board impact	38 kJ 2) 3)	ULS or ALS 1)	0^o to 20^o horizontal
1) ULS or ALS depending on trawl interference frequency at field. ALS applies if frequency is less than 0.01x year. 2) Applies for largest type of trawl gear currently used in the North and Norwegian seas. 3) Applies for standard tubular framework structure.			

Table 5-2 Generic design loads requirement [19]

The design loads were calculated based on a model trail in which a trawl board of 4500 kg and a clump weight of 6000 kg moving at a speed of 2.8 m/s, at a water depth of 100m. From the tables above, one can see that Statoil accommodates the increase in trawl weights by multiplying the design loads for trawl board pull-over by a factor of 1.5 and trawl board impact by a factor of 2.9.

Chapter 6 Experiment

This experiment was conducted in the instrumentation laboratory at the University of Stavanger. The steel rods and plates required for the construction of the main apparatus in this experiment were gathered from the Department of Material Science´s workshop at the University.

This experiment was undertaken to investigate the effect of water trapped in the pipe as well as water surrounding the pipe, on the amount of Impact energy absorbed by the pipe. In order to reach this purpose, a hammer (´chested-hammer´) was built from scratch with the ability to deliver a blow that lasts a hundredth of a second, fulfilling the definition of an impact.

6.1 Apparatus

6.1.1 The Hammer

The impact apparatus consist mainly of five parts (fig 6.1 below):

- A support that is fixed and non-rotational such that the pipeline can be fully clamped in it.
- A base plate structure that carries the support and provide a foundation for the top structures.
- Four steel pipes acting as a structural pillar: transferring the weight of the top structures to the foundation as well as providing enough stiffness to withstand both horizontal and vertical movement of the whole structure.
- A top structure that accommodates the striker.
- A striker, with a top protruded end for the addition of weights and a bottom smooth end meant to indent the pipe. The striker and its auxiliary parts are attached to the top plate in such a way that they are adjustable. This is important because in this experiment, the striker is designed to strike the mid-span of the pipeline.

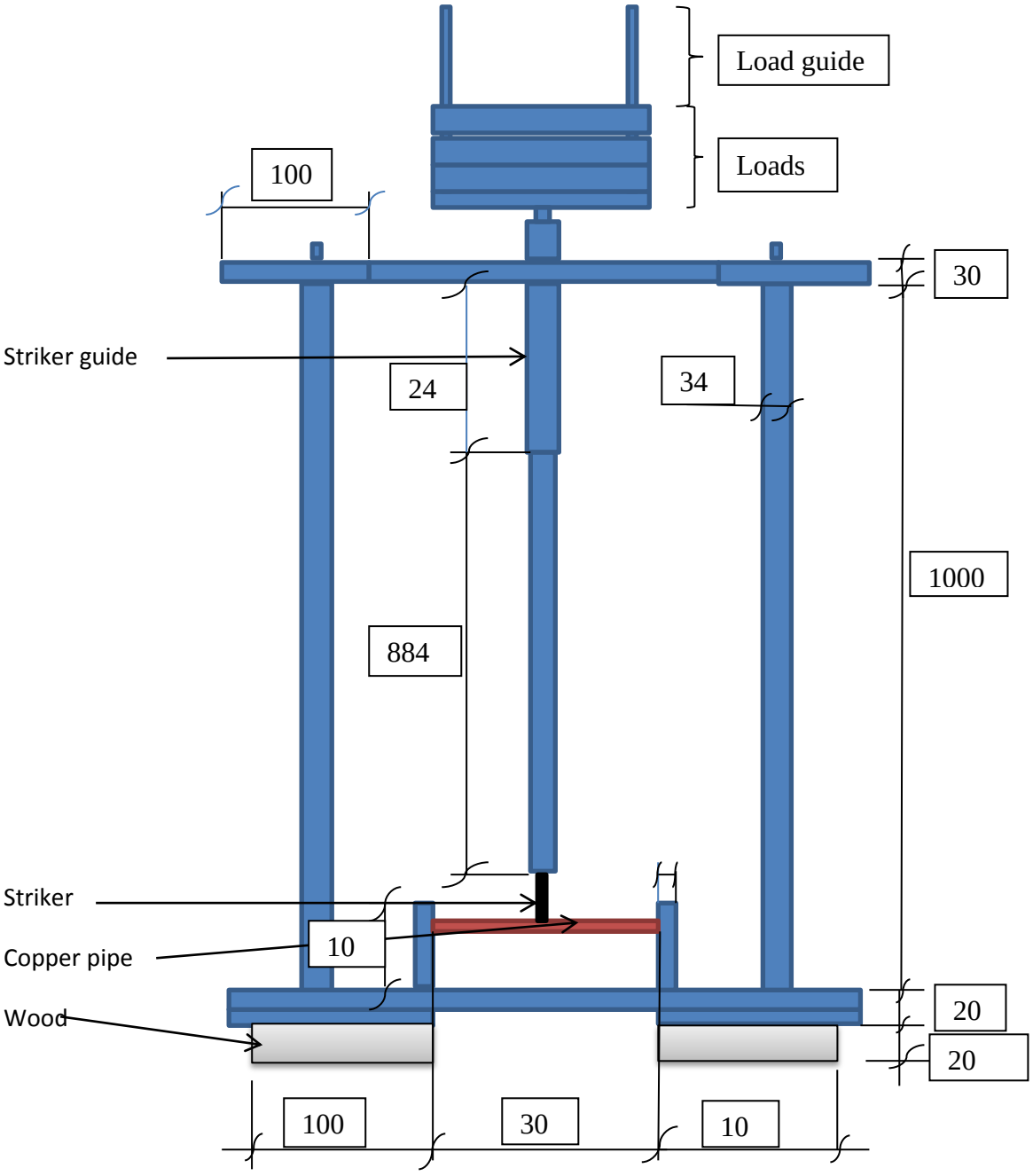

Figure 6-1 The impact hammer and its dimensions(mm)

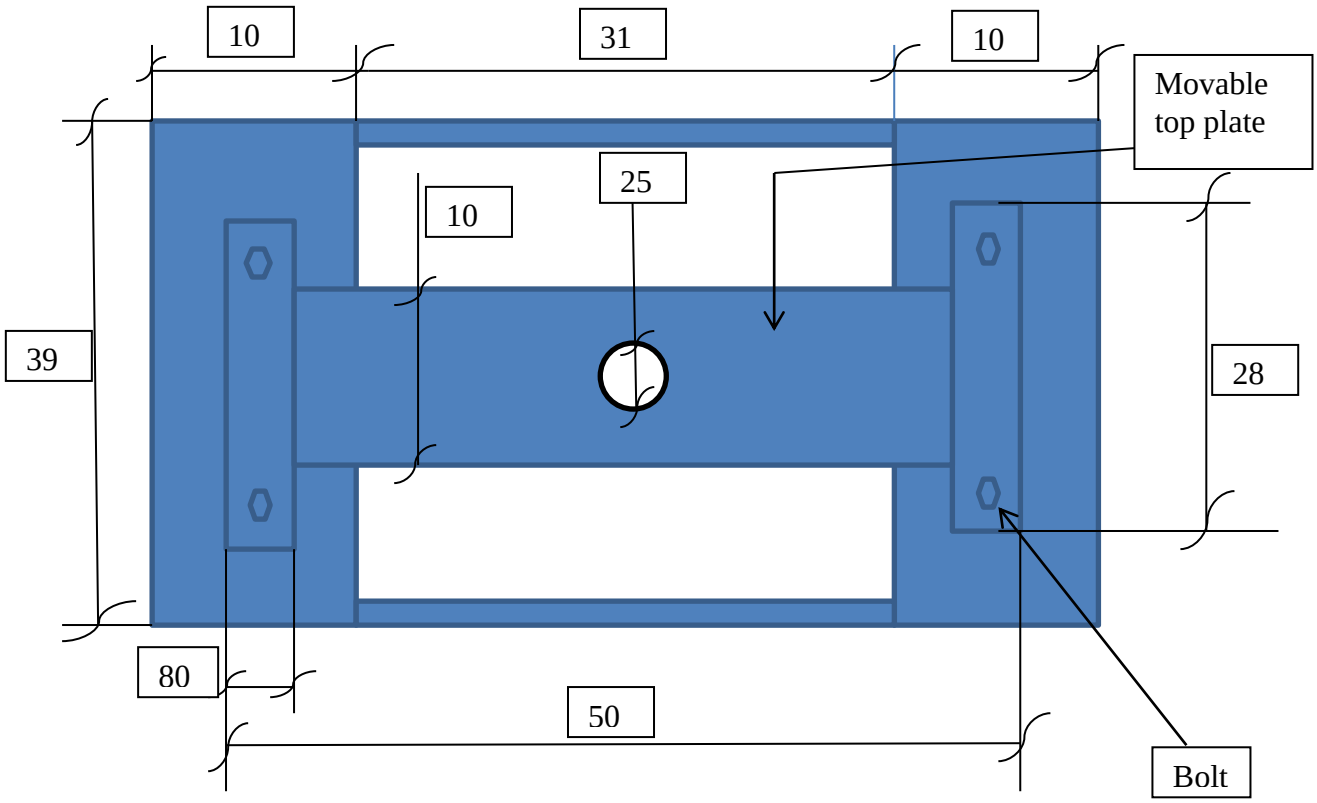

Figure 6-2 Detailed diagram of the top structure and its dimensions (mm)

Figure 6-3 The impact hammer

6.1.2 The Pipeline

The pipeline is made up of half-hard copper having the following qualities:

- Tensile strength, σ_t: min 310 N/mm^2
- Yield strength, σ_y: min 280 N/mm^2
- Young`s Modulus E: 1.2E11 N/m^2
- Density ρ: 8.94 kg/dm^3
- Poisson's ratio, ν: 0.3
- Coefficient of Linear Thermal Expansion, α: 17E-6
- Outer diameter, OD: 15 mm
- Inner diameter, ID: 13 mm
- Wall thickness, T: 1 mm

Three copper pipes of length 2000mm each was cut into fifteen pipes. Each of the fifteen pipes had a length 320mm. The pipes were divided into a three groups:

- Group 1 consist of five empty pipes.
- Group 2 consist of five water-filled pipes. The water is trapped in the pipe by a stopper, place at both ends. This group will be tested in air.
- Group 3 consist of five water-filled pipes. In this case, the pipes will be tested in water.

6.1.3 Water Tank

The water tank used in this experiment is a large rectangular bowl of dimensions 720 mm x 650 mm x 170 mm.

6.2. Sensors and Data Acquisition

In order to get an inside into the strain evolution at the mid-span for the three pipe categories (mentioned above), a strain gage was placed at the tensioned-end of a pipeline from each category.

6.2.1 Strain Gages

The strain gages of the type K-LY43-6/120 were used in this experiment. Given that the striker will hit the pipe at the mid-span, this point is chosen as the point where the strain gages will be installed. This is because; this section will experience the greatest strain as compared to other sections along the pipeline.

The installation of the strain gage was carefully done. Care was taken to ensure that the strain gages are attached at the midpoint of the pipeline and that that the gages are parallel to the pipe axis thereby eliminating reading errors that might originate from slight angular deviation of the gages from the pipe´s axis.

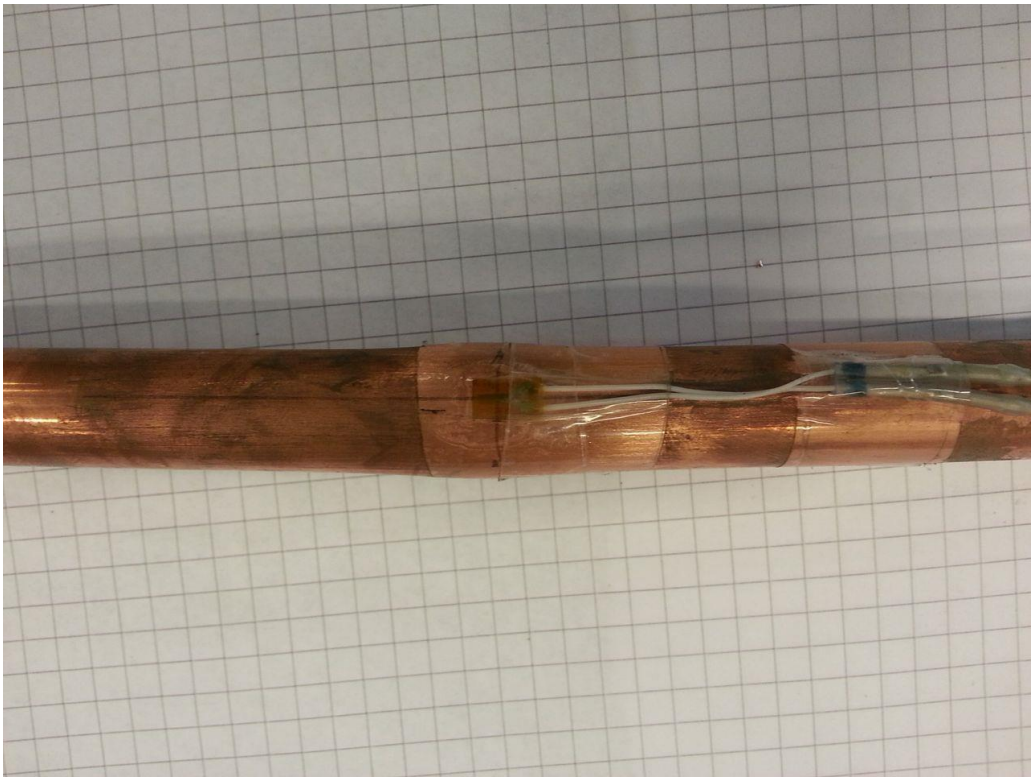

Figure 6-4 Illustration of a strain gage attached at a pipe's mid-span

Two strain gages are required for each pipe i.e. an active and a dummy gage. The active gage is attached to the pipe that will be stroked while the dummy gage is attached to the dummy pipe. The use of the dummy is to compensate for the effect of temperature variation on the strain gage readings. The six wires of both strain gages (2 greys and 1 red for each gage) are connected to a 15-pin port as shown below:

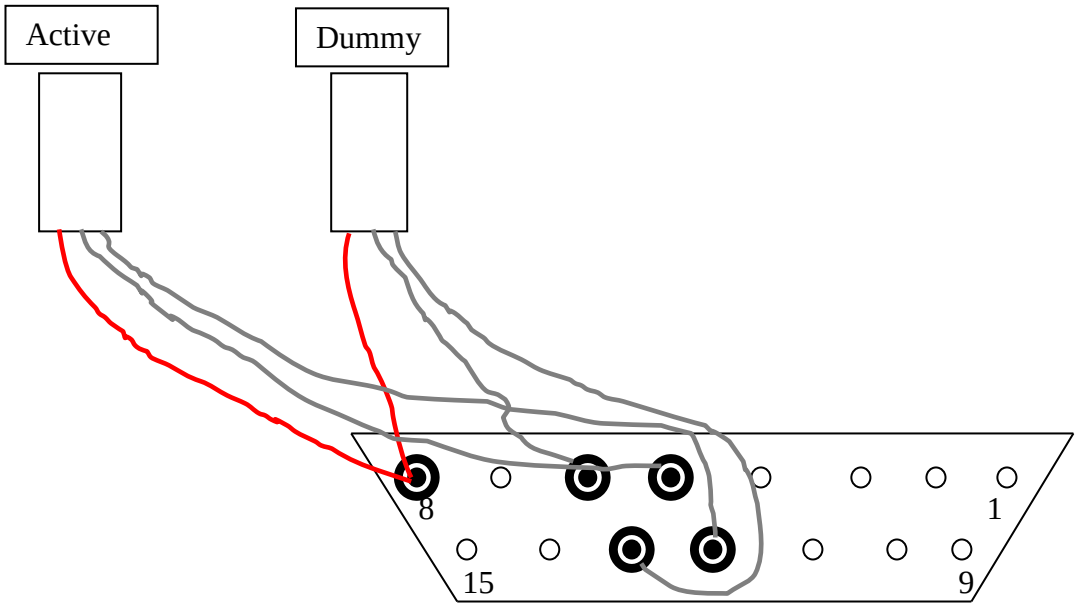

Figure 6-5 Illustration of the mode of connection between the two strain gages and a 15-pin port

6.2.2 Spider8 and PC

The 15 –pin port is then connected to a hardware called Spider8. Spider8 amplifies the signal from the sensors and sends it to the computer connected to it.

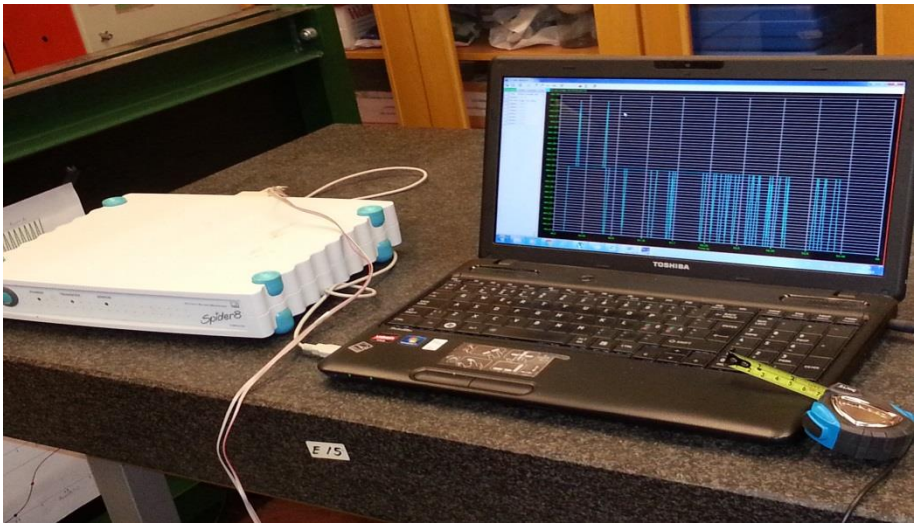

Figure 6-6 Spider 8 hardware (white box to the left) connected to a PC

The computer runs a program called Catman Basic. This program interprets the data from the Spider8 and output the strain in μm/m against time. The program further makes it possible to calibrate the strain gage. In this experiment, a gage factor of 2.02 was chosen. This value is recommended for these strain gages.

6.2.3 Distance Measuring Tools

The length, thickness and diameter of the original and deformed pipe were all measured using a meter rule and a calliper.

6.3 Procedure

As mentioned earlier, the pipes are grouped into three: empty pipes in air, water-filled pipes in air and water-filled pipes in water. Before starting the experiment, a strain gage is attached to the mid-span of the pipe. The experiment is conducted for each group with slight modifications as explained below:

6.3.1 Group I - Empty Pipes in Air

The first group of five empty pipes are differentiated with numbers. The pipe, to which a strain gage is attached to, is tested first.
The hammer is placed on a level floor with two pieces of wooden slabs attached underneath. This levels the bottom steel plates which became curved after welding.

The pipe is then placed at the support and adjusted such that the midpoint of the pipe coincides with the midpoint between the supports and the attached strain gage should be at the bottom of the pipeline. The dummy strain gage is placed on the table.

The 15-pin port is then connected to the Spider8 which is then connected to a computer .The Catman program is started and configured as detailed in appendix III.

The striker is then inserted inside the guide [see figure 6.1] and the top movable plate together with the striker are adjusted until the striker is located vertically above the midpoint of the supported pipe. The movable plate is then fixed at this position. Weights are added to the striker until the total weight including the weight of the striker reaches 94.37 N.
The striker is then lifted to a height of 0.56 m and this point is set as a reference point.
At this point, the strain readings are initialized in the Catman program. The striker is then dropped from the above mentioned height such that it falls freely, attaining a maximum velocity of 3.32 m/s (see appendix A1) striking the fully clamped pipe at its midpoint.

The weights were chosen appropriately after many successive tests. This is particularly important as we do not want the pipe to be stroke twice i.e. at the first strike, the pipe will deform in such a way that a rebound will not strike that pipe.

After the impact, data acquisition is switched off .The deformed pipe is then retrieved for measurements. The pipe is sectioned through the midpoint of the indented surface. The maximum width of the deformed section (D_m) and the local permanent thickness of the deformed cross-section (T_r) are then measured using a calliper.

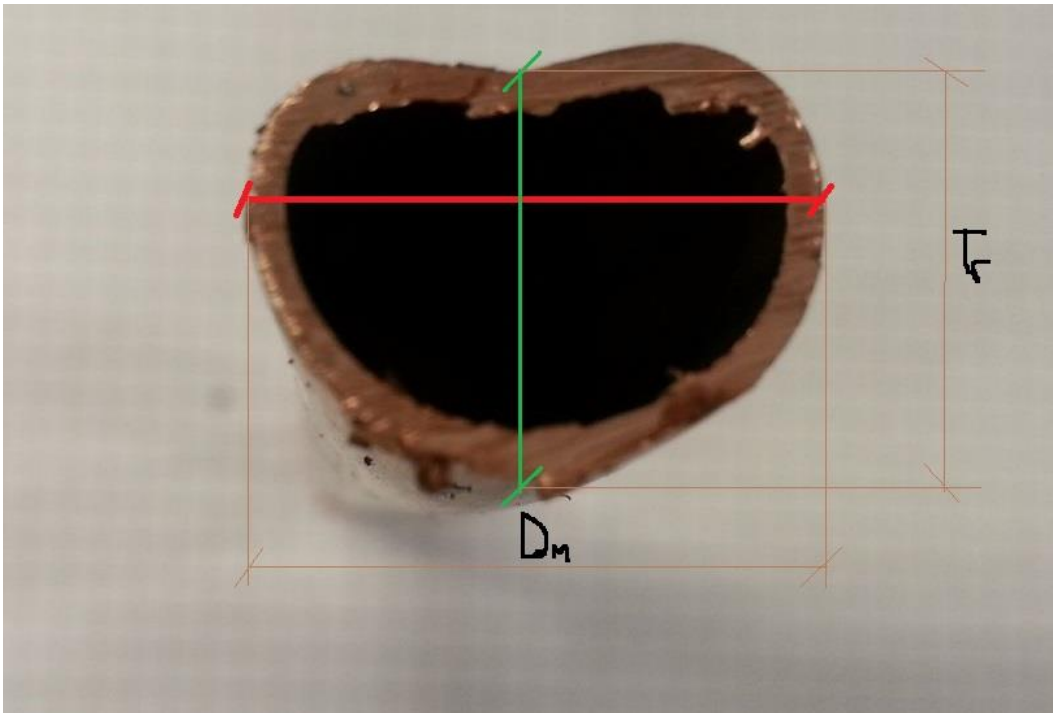

Figure 6-7 Measured parameters for the deformed cross-section

The experiment is repeated for the remaining four empty pipes in the group without strain gage and the weight of the striker is increased by 14N for each pipe.
The Striker is raised to the same height (0.56 m) and released from rest. The pipes are sectioned and values for D_m and T_r are measured.

6.3.2 Group II - Water-filled Pipe in Air

In this group, the pipes are filled with water and sealed at both ends using a plastic stopper. The seal is firmed, preventing leakage of water from the pipe before, during and after impact. The first test is done with a pipe to which a strain gage is attached. The same procedures mentioned above for group I are followed and the various values of D_m and T_r measured.

6.3.3 Group III - Water-filled Pipe in Water

The pipes in this group are filled with water and sealed at both ends as well. The first test is done on the pipe having a strain gage attached to it. The pipes are placed on support and the hammer is then placed in a rectangular bowl and water is poured in the bowl until the pipe is submerged. The amount of water is just sufficient to submerge the pipe.
The reason for this is to avoid hydrodynamic forces acting on the hammer, thereby affecting its speed and weight.

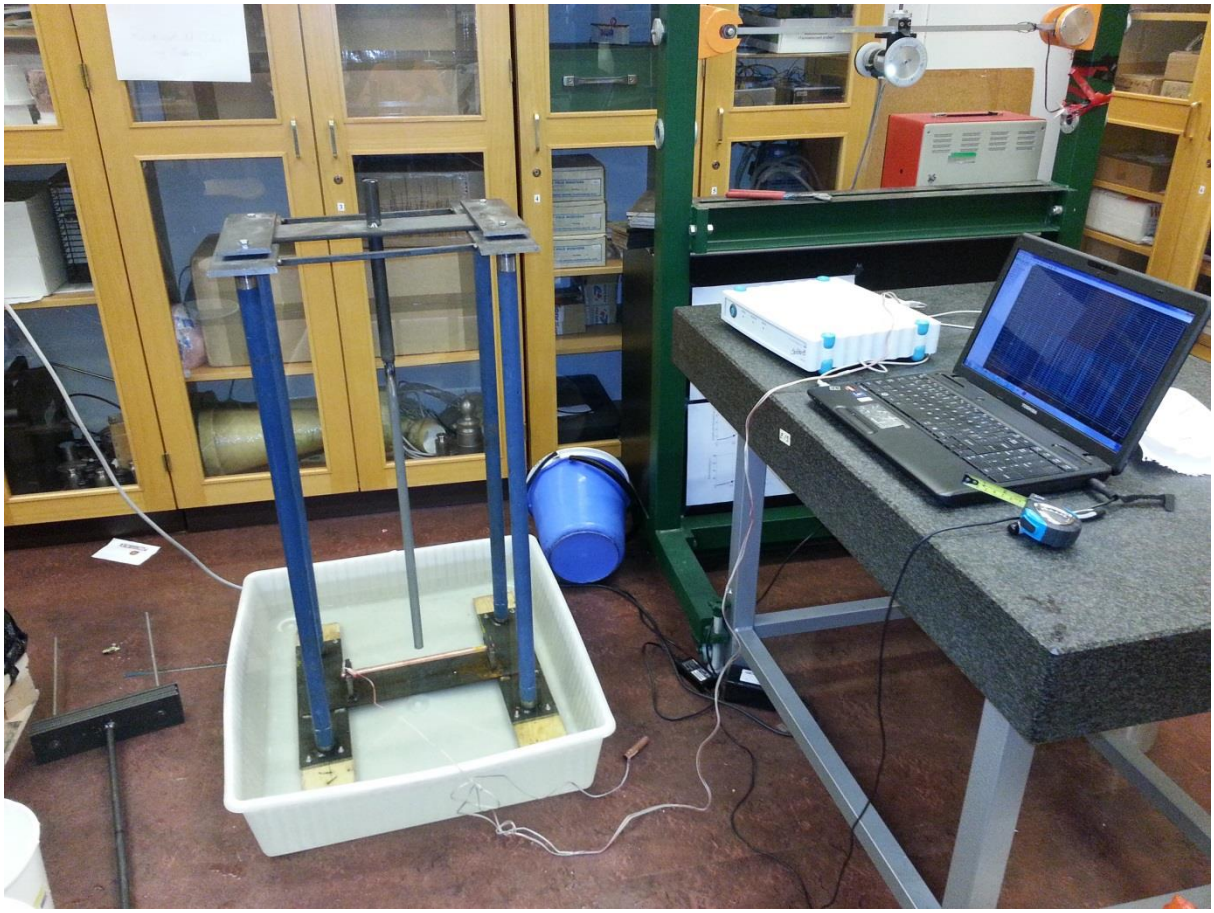

Figure 6-8 Experimental setup for impact test in water

Except for the water tank, the same procedure mentioned above (Group II) is followed, and the measured values for D_m and T_r for this group are recorded.

CHAPTER 7 Results

The results for each group are presented below in both tabular and graphical forms. The tables contain the obtained values of D_m ,T_r and W_f for all the pipes in the first group and the calculated values for the local and global plastic deformation energies according to the above mentioned theories.

7.1 Empty Pipes Tested in air

The table below show the measured values of D_m, T_r and W_f , measured from the deformed cross-section of the pipes after impact with the striker. From the table, it is observed that the maximum permanent transverse displacement (W_f) increases with increase in weight (or kinetic energy) of the striker. This is to be expected as the size of the dent on the pipe will depends on the striker´s kinetic energy.

In contrary to the transverse displacement, both the width of the cross-section and the residual thickness decrease with increasing striker energy. This tendency can be best explained by the fact that for an empty pipe, most of the plastic energy is used in indenting. Therefore less plastic energy is used in deforming the whole cross section. This phenomenon becomes significant at higher energies.

Empty pipes in air				
Element number	Weight of Striker(N)	Maximum permanent width across the deformed section (D_m) in mm	Residual thickness across the deformed profile (T_r) in mm	Maximum permanent transverse displacement (W_f) in mm
1	94.372	16.68	11.73	3.28
2	108.106	16.52	11.80	3.21
3	121.840	16.58	11.59	3.42
4	135.574	16.56	11.51	3.50
5	149.308	16.46	11.45	3.56

Table 7-1 Values measured from the deformed cross-sections for the empty pipes tested in air

Using the equations (9), (11), (12), (16), (17) and (20) from the theory of Ellinas and Oliveira mentioned above, the values of the local and permanent global displacements, absorbed local indentation and global deformation plastic energies were computed respectively(Table 7-2).

The local displacement increases with increase in kinetic energy i.e. at higher kinetic energy, the pipe exhibits larger local displacement. However, the global displacement exhibits overall diminishing values as the kinetic energy of the striker increases. These values are presented in the table below:

Empty pipes in air								
Element Number	Kinetic energy of Striker (J)	W_f (mm)	W_l (mm)	W_g (mm)	Energy absorbed plastically during local indentation (E_{pl}) and global deformation (E_{gl}). In Joules [J]			
					Ellinas and Walker		Oliveira,Wierzebicki and Abramowicz	
					E_{pl}	E_{gl}	E_{pl}	E_{gl}
1	52.848	3.28	2.581	0.6991	7.317	-0.054	5.003	0.984
2	60.539	3.21	2.532	0.6784	7.109	-0.058	4.860	0.955
3	68.231	3.42	2.758	0.6617	8.084	-0.061	5.528	0.931
4	75.922	3.50	2.853	0.6474	8.502	-0.063	5.813	0.911
5	83.613	3.56	2.940	0.6203	8.895	-0.068	6.082	0.873

Table 7-2 Calculated values of local and global displacements and their associated plastic energies for the empty pipes tested in air

The figure below (figure 7.1) shows how the strain varies with time. The striker stroke the pipe at time 440 second and the impact lasted about one hundredth of a second. The pipe´s strain reached a value of 0.0048.

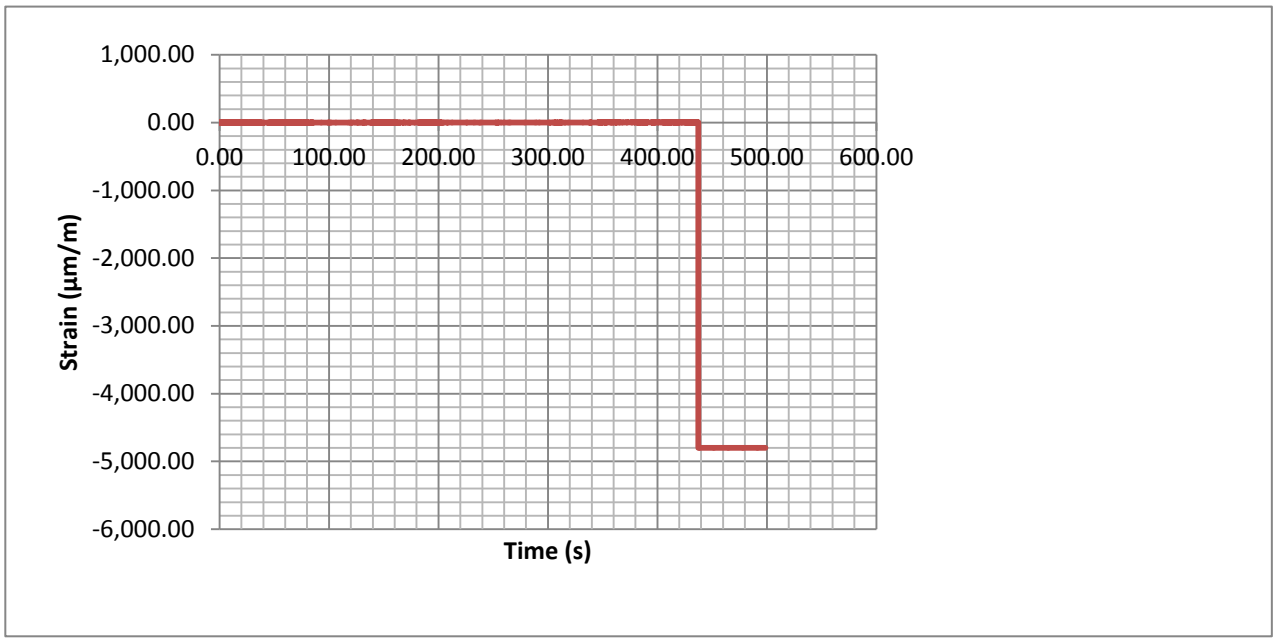

Figure 7-1 Strain variation with time for the impact load at the mid-span of an empty pipe in air

The maximum yield strain calculated in appendix A2 is 0.002583. Therefore as the pipe yields, it experience an additional strain of 0.002217 at the midpoint where the striker stroke.

7.2 Water-filled Pipes Tested in Air

Water-filled pipes in air				
Element number	Weight of Striker(N)	Maximum permanent width across the deformed section (D_m) in mm	Residual thickness across the deformed profile (T_r) in mm	Maximum permanent transverse displacement (W_f) in mm
1	94.372	16.53	11.92	3.09
2	108.106	16.52	11.82	3.19
3	121.840	16.63	11.70	3.31
4	135.574	16.64	11.58	3.43
5	149.308	16.71	11.54	3.47

Table7-3 Values measured from the deformed cross-sections for the water-filled pipes in air

It can be observed here that the transverse displacement and the maximum width of the cross-section increase with increasing striker energy while the residual thickness across the deformed section decreases.

The increase in maximum permanent width across the deformed section as the striker´s weight increases signifies that a considerable amount of plastic energy has been used to deform the cross section and hence a relatively low energy will be used for indenting.

Water-filled pipe in air								
Element Number	Kinetic energy of Striker (J)	W_f (mm)	W_l (mm)	W_g (mm)	Energy absorbed plastically during local indentation (E_{pl}) and global deformation (E_{gl}). In Joules [J]			
					Ellinas and Walker		Oliveira,Wierzebicki and Abramowicz	
					E_{pl}	E_{gl}	E_{pl}	E_{gl}
1	52.848	3.09	2.393	0.6967	6.534	-0.054	4.467	0.981
2	60.539	3.19	2.509	0.6811	7.013	-0.057	4.795	0.958
3	68.231	3.31	2.624	0.6857	7.503	-0.056	5.130	0.965
4	75.922	3.43	2.758	0.6719	8.084	-0.059	5.527	0.946
5	83.613	3.47	2.790	0.6802	8.223	-0.057	5.622	0.957

Table7-4 Calculated values of local and global displacements and their associated plastic energies for the water-filled pipes tested in air

From the figure below (fig 7.2), it can be seen that the strain in the midsection of the pipe attained the value 0.004. The section experienced an additional strain of value 0.001417 well beyond its elastic region.

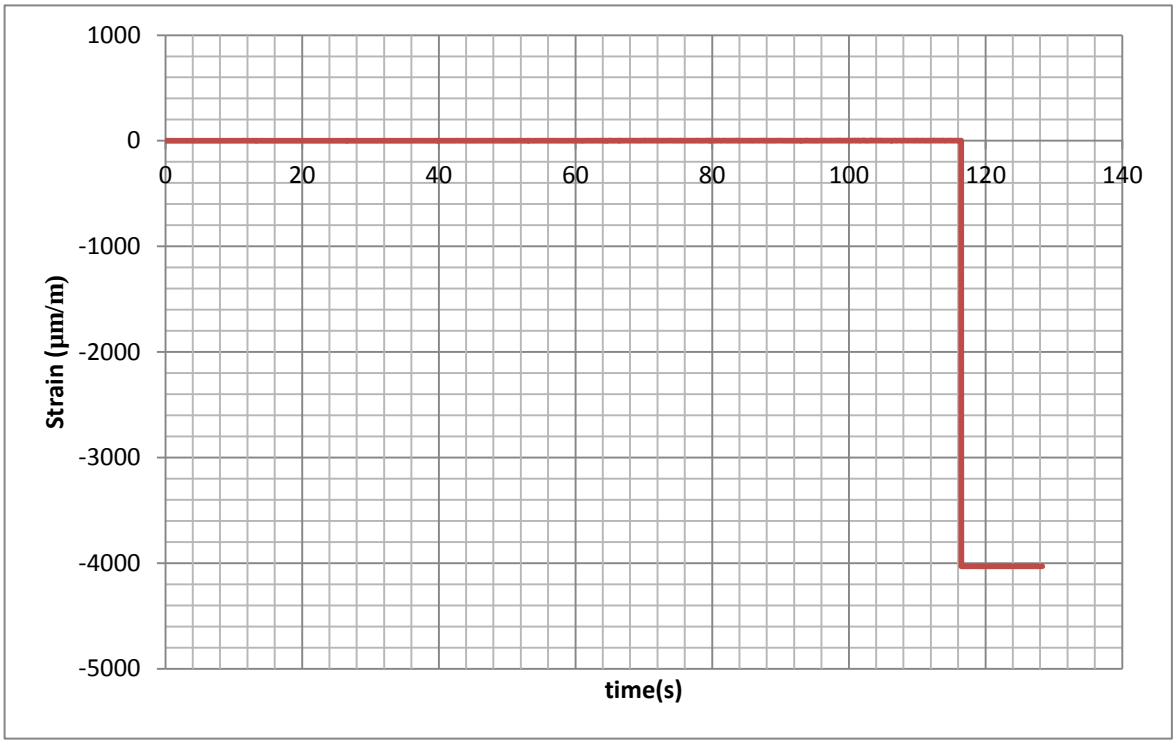

Figure 7-2 Strain variation with time for impact at mid-span of a water-filled pipe in air

7.3 Water-filled Pipes Tested in Water

The trend in the values of D_m , T_r and W_f are quite similar to the case above where the water-filled pipes were tested in air

Water-filled pipe in water				
Element number	Weight of Striker(N)	Maximum permanent width across the deformed section (D_m) in mm	Residual thickness across the deformed profile (T_r) in mm	Maximum permanent transverse displacement (W_f) in mm
1	94.372	16.48	11.94	3.07
2	108.106	16.53	11.83	3.18
3	121.840	16.62	11.62	3.39
4	135.574	16.60	11.57	3.44
5	149.308	16.70	11.47	3.54

Table 7-5 Values measured from the deformed cross-sections for the water-filled pipes tested in water

Water-filled pipe in water								
Element Number	Kinetic energy of Striker (J)	W_f (mm)	W_l (mm)	W_g (mm)	Energy absorbed plastically during local indentation (E_{pl}) and global deformation (E_{gl}). In Joules [J]			
					Ellinas and Walker		Oliveira,Wierzebicki and Abramowicz	
					E_{pl}	E_{gl}	E_{pl}	E_{gl}
1	52.848	3.07	2.380	0.6903	6.479	-0.055	4.430	0.972
2	60.539	3.18	2.496	0.6843	6.958	-0.057	4.757	0.963
3	68.231	3.39	2.717	0.6733	7.902	-0.059	5.403	0.948
4	75.922	3.44	2.777	0.6629	8.167	-0.061	5.584	0.933
5	83.613	3.54	2.871	0.6695	8.583	-0.059	5.868	0.942

Table 7-6 Calculated values of local and global displacements and their associated plastic energies for the water-filled pipes in water

From figure 7.3, the water-filled copper pipe tested in water reached a strain value of 0.00440. This corresponds to an additional strain value of 0.001817 beyond the maximum elastic strain.

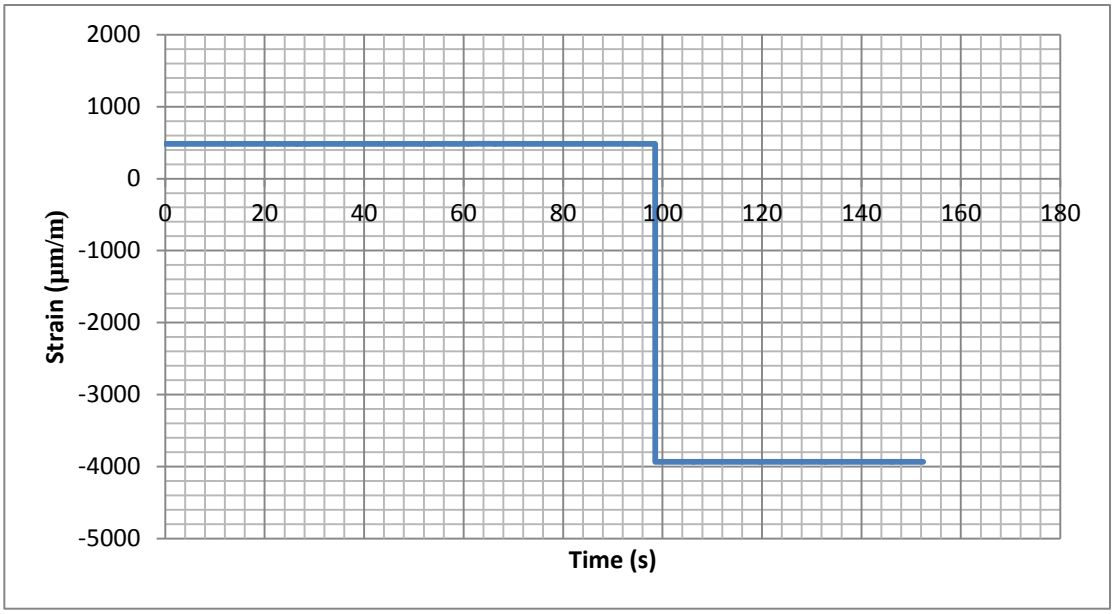

Figure 7-3 Strain variationwith time for impact at mid-span of a water-filledpipe in water

7.4 Comparisons of the Results

In order to fully determine the effect of water trapped in the pipe as well as surrounding the pipe, values of the local displacement, maximum permanent transverse displacement, maximum width of the deformed cross-sections, local permanent thickness of the deformed cross-section and the local indentation energy absorbed plastically for the various groups will be compared

7.4.1 Local Displacement

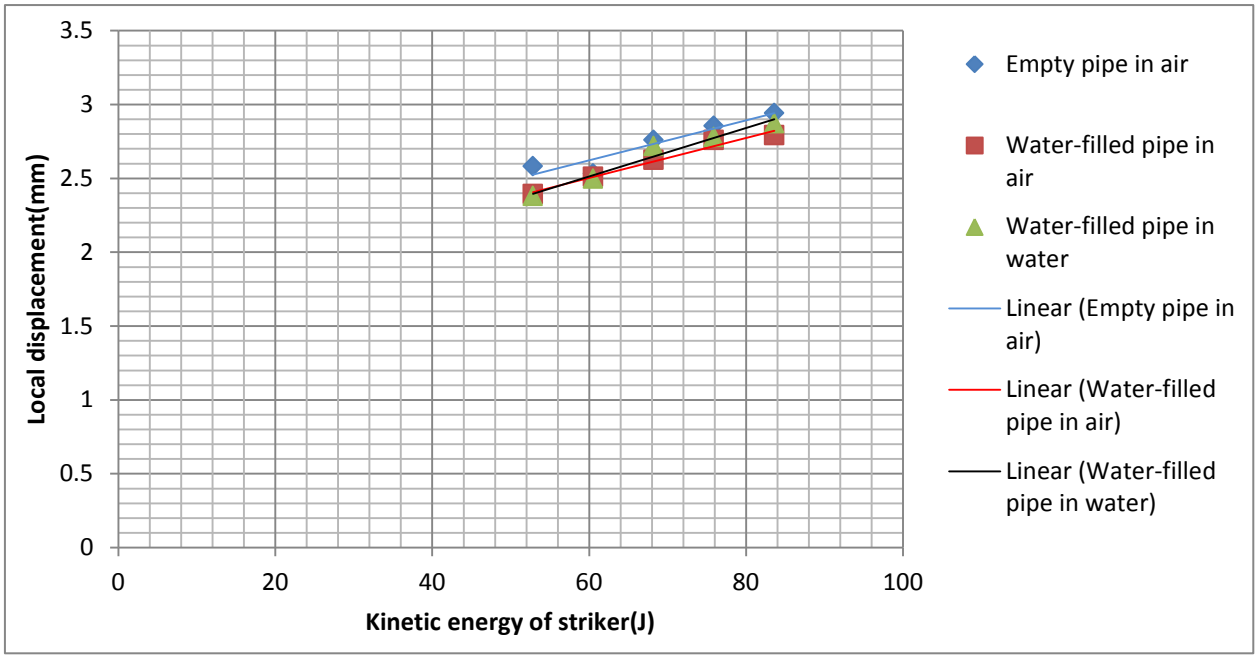

Figure 7-4 Variation of the local displacement with kinetic energy of the striker for the various groups

From the figure above (figure 7-4), it can be seen that the overall tendency for all the groups is an increase in local displacement for increase in the striker´s kinetic energy. However, there is a distinction between the various groups in the sense that, the empty pipes in air show larger local displacement at each kinetic energy than the water-filled pipes in air and in water.

The water-filled pipes in air and those in water, show similar behavior with increase in the striker´s kinetic energy. Their local displacements are somewhat much closer to each other if we neglect the slight variation in the decimals.

The values form a cluster as the kinetic energy becomes very high. Based on this trend, one can extrapolate that at very high kinetic energy of the striker (far greater than 80 J) the local displacements for the three groups converge.

7.4.2 Maximum Permanent Transverse Displacement

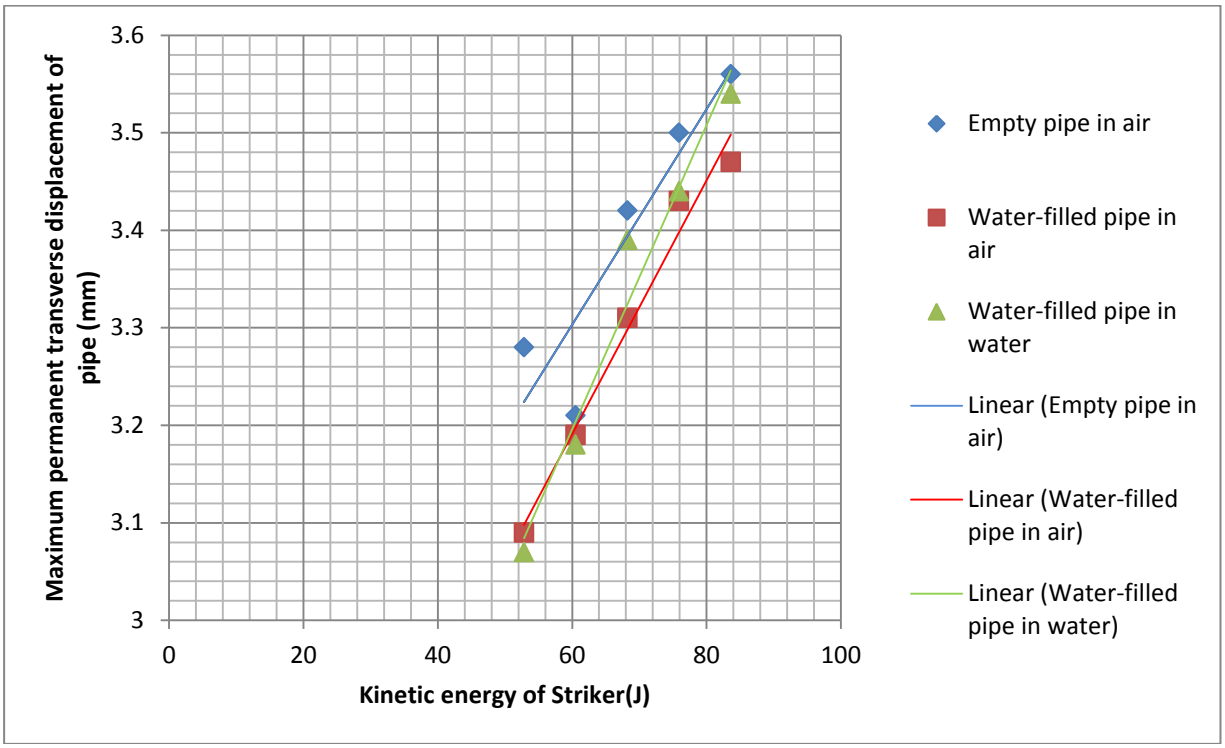

Figure 7-5 Variation of the maximum permanent transverse displacement with kinetic energy of the striker for the various groups

The empty pipes tested in air, show larger transverse displacement than the water-filled pipes tested in both air and water at each kinetic energy of the striker.

Both water-filled pipes show relatively similar (within acceptable limits) transverse displacement, although their trends seem to deviate from a common path as the energy of the striker increases.

7.4.3 Maximum Width of the Deformed Cross-Section

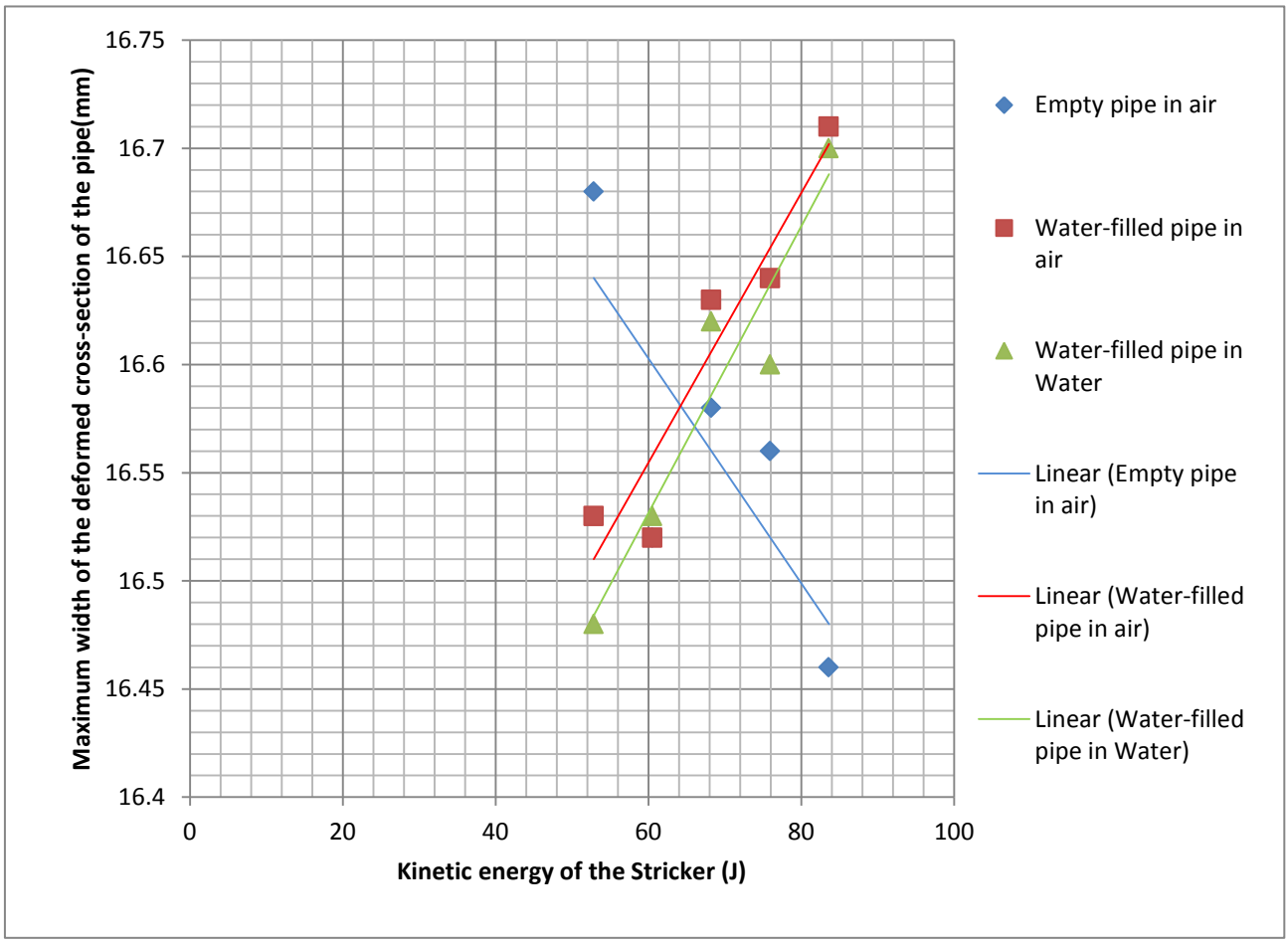

Figure 7-6 Variation of the maximum width of the deformed cross-section with kinetic energy of the striker for the various groups

From figure 7-6, the following trends can be deduced:

- For the empty pipes tested in air, the maximum widths of the deformed cross-sections are large for low energies and small for high energies.

- Both the water-filled pipes tested in air and water has maximum width of deformed cross-sections that increase with increase in the striker´s kinetic energy.

- For most kinetic energy, the water-filled pipes tested in air show a large width of the deformed cross-sections than the others, although there is not much difference when compared with the water-filled pipes tested in water. This is true for most of the results.

7.4.4 Local Permanent Thickness of the Deformed Cross-Section

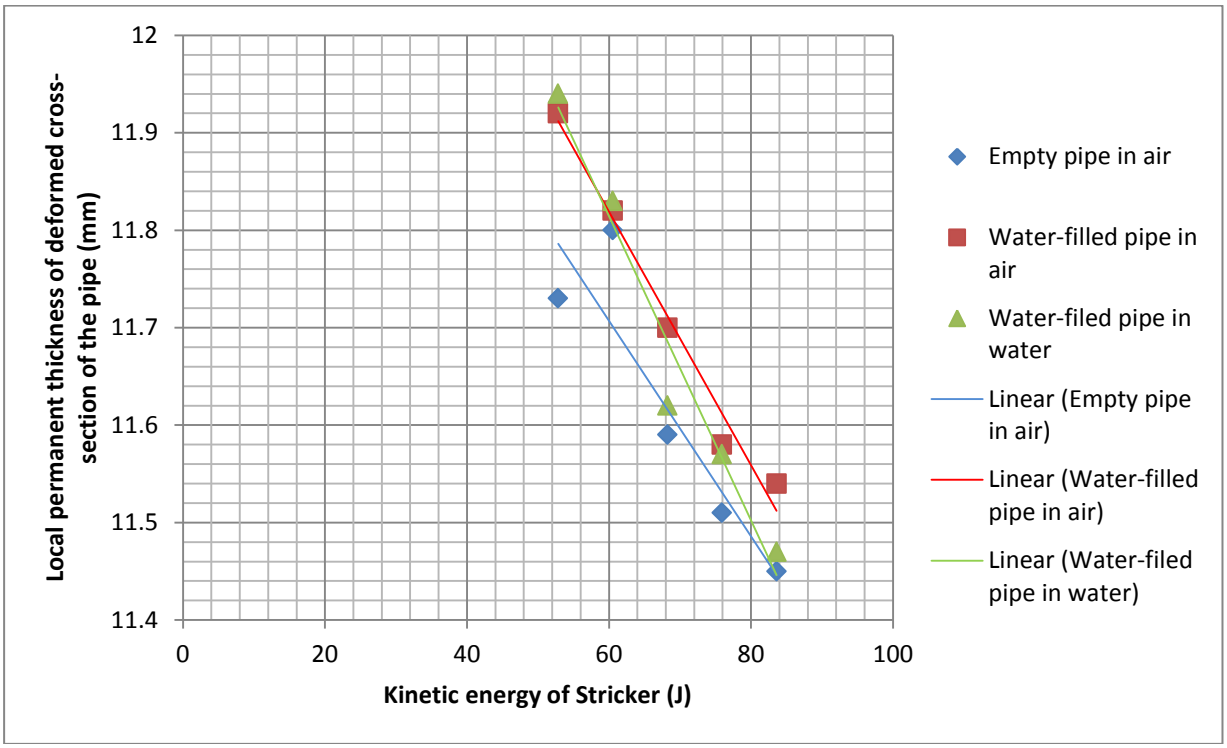

Figure 7-7 Variation of the local permanent thickness of the deformed cross-section with kinetic energy of the striker for the various groups

For all three groups, the local thicknesses of the deformed cross-sections decrease with increase in kinetic energy. This is expected given that the dents somewhat increase in depth as the impact load increases.

The water-filled pipes tested in air and in water, have larger thickness of the deformed cross-sections than the empty pipes in air for the same energy of the striker.

7.4.5 Local Indentation Energy Absorbed Plastically-Ellinas Theory

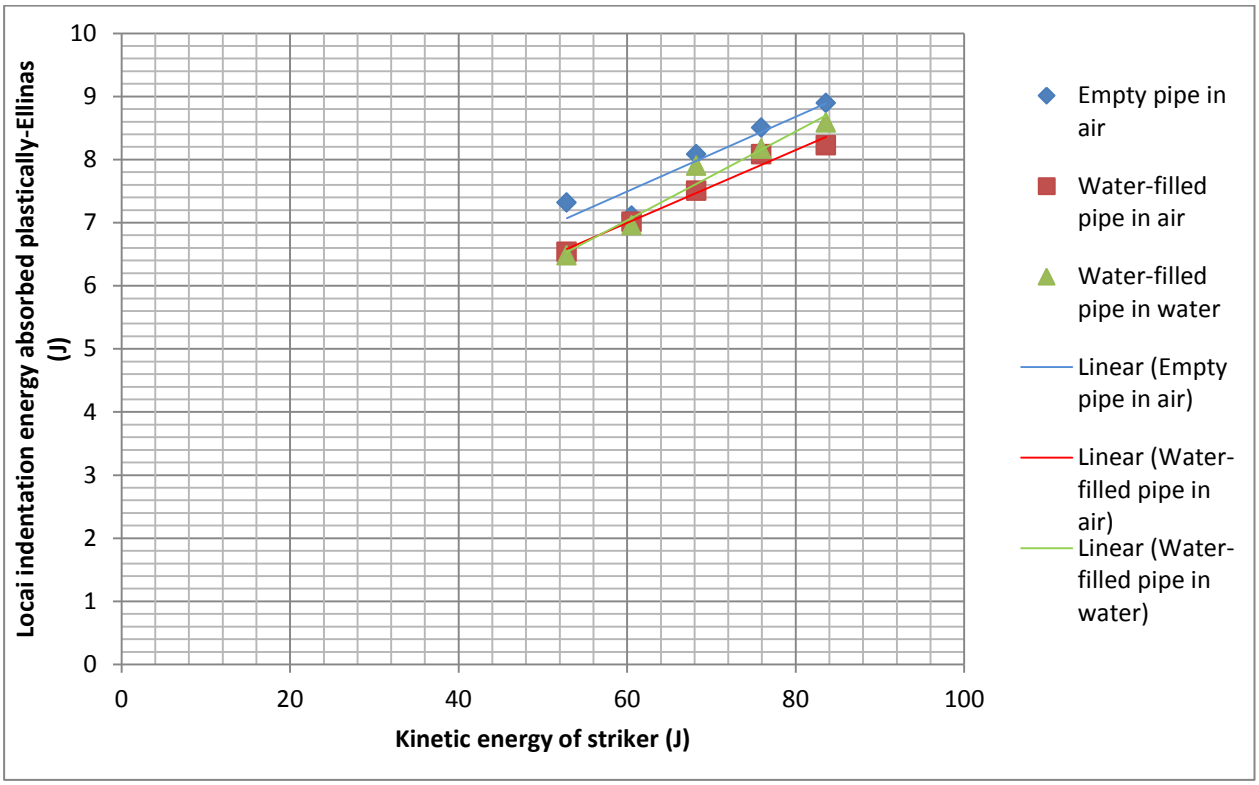

Figure 7-8 Variation of the local indention energy absorbed plastically with kinetic energy of the striker for the various groups using Ellinas and Walker's theory

The figure above (figure 7-8) shows how the indentation plastic energy varies with the impact energy (energy of the striker). All the groups show an increase in the absorbed plastic energy with increasing impact energy. The following points can be deduced:

- The empty pipes tested in air generally absorbed the highest amount of indentation plastic energy for any given amount of impact energy.
- The water-filled pipes tested in air and in water, absorbed to some extend almost the same amount of indentation plastic energy for the same impact energy.

7.4.6 Impact Energy Absorbed According to DNV versus Impact Energy Absorbed using Ellinas and Walker's Theory

The following assumptions are made:

- The strain maxima occur around the region of the dent, spanning a length twice the diameter of the striker so that we can neglect the elastic energy absorbed elsewhere along the pipe. This is a reasonable assumption given that the rest of the pipe remains intact after impact.
- The striker models the impact from a trawl board.

From the above assumptions, the total elastic strain energy (W_s) and the impact energy absorbed (using DNV-RP-F111) can be calculated as shown in Appendix A3 and A4.
The total impact energy absorbed by the pipe is then given by:

$$E_T = W_s + E_{pl} + E_{gl}$$

Where

E_{pl} = Energy absorbed plastically during local indentation
E_{gl} = Energy absorbed plastically global deformation

Weight of Striker(kg)	Impact energy absorbed (J) (DNV-RP-F111)	Total energy impact energy absorbed (J) Ellinas and Walker theory					
		Group 1		Group 2		Group 3	
	E_{T-DNV}	E_T	% of E_{T-DNV}	E_T	% of E_{T-DNV}	E_T	% of E_{T-DNV}
9.620	20.030	8.963	44.75	8.180	40.84	8.124	40.56
11.020	22.945	8.751	38.14	8.656	37.72	8.601	37.49
12.420	25.860	9.723	37.59	9.147	35.37	9.543	36.90
13.820	28.775	10.139	35.24	9.725	33.79	9.806	34.08
15.220	31.690	10.527	33.22	9.866	31.13	10.224	32.26

Table 7-7 Total impact energy absorbed for the various striker weights

From the table above, it can be deduced that the total impact energy absorbed using Ellinas and Walker´s theory is on average **37.79%** of the calculated impact energy absorbed using DNV simplified formulas. This is true for the empty pipes tested in air.
Therefore the calculate impact energy absorbed by the pipes using DNV codes is **2.65** times larger than the energy calculated, using Ellinas and Walker´s theory.

It also follows that, for the water-filled pipes tested in water, the calculated impact energy absorbed is **35.77%** of the energy calculated with DNV codes, implying that DNV values are **2.79** times greater.

The water-filled pipes tested in water absorbed impact energy that is **36.26%** of the calculated DNV value, making the DNV value **2.76** times greater.

The relationship between the impact energies calculated using the DNV codes and those calculated using the Ellinas and Walker´s theory (which as a matter of fact agrees with many data from experiments) can be expressed as shown below:

$$\mathbf{E_{T\text{-}DNV} = \mathit{f}\ E_T}$$

Where

$E_{T\text{-}DNV}$ = calculated impact energy using DNV-RP-F111

E_T = calculated impact energy using Ellinas and Walker´s theory

f = 2.73 the average of {2.65, 2.79, 2.76}.

The factor f determine the level of conservatism

Chapter 8 Conclusion and Recommendation

8.1 Summary and Conclusion

In this thesis, the deformed geometry of the pipes cross-sections have been idealized and parameters such as the maximum width, permanent thickness etc. have been measured and used as inputs in accepted theories.
The objective of this thesis has been to determine the effect of the water trapped in the subsea structure (in this case a pipeline) and the surrounding water on the amount of impact energy absorbed by the structure.

Many assumptions that can have an effect on the values obtained in this work have been made. These assumptions are presented below:

- The pipeline is perfectly clamped at the support in such a way that there is no displacement and yielding at the support.

- The strain in the pipeline during impact is at its maximum at the vicinity of the point of contact with the striker i.e. up to a circular region of diameter equal to the striker´s diameter, measured from the striker´s axis.

- The pipelines materials of the same quality such that they attain the same maximum elastic strain.

- Negligible friction between the striker and the guide.

- Negligible amount of energy lost during impact as sound and heat.

Some of these assumptions are highly unachievable. For example, the pipeline experiences to some extend plastic deformation at the support and the strain wave propagates throughout the pipeline not at the vicinity of the impact point.

From the results obtained from the test, the following observations are made:

- The empty pipes tested in air exhibit the following:

    - The largest local displacement.
    - The largest transverse displacement.
    - Overall smaller width of deformed cross-section.
    - Lesser thickness of the deformed cross-sections.
    - Greatest amount of indentation plastic energy absorbed for any given impact energy.

- ❖ The water-filled pipes tested both in air and water exhibits similar properties outlined below:

    - Smaller local displacement.
    - Larger width of deformed cross-sections.
    - Largest thickness of the deformed cross-sections.
    - Lesser amount of indentation plastic energy for any given impact energy.

Based on these observations, it is clear that there is a significant effect on the pipeline´s resistance to deformation due to impact when water is trapped inside the pipeline. The water-filled pipeline exhibits lesser indentation and plastic energy absorbed and hence offers somewhat higher resistance to damage due to impact with trawl gear.

A plausible explanation to this behavior is that during impact, the initially unpressurised water-filled pipeline becomes pressurized as the incompressible fluid (water) is pushed away during impact from the point of contact. An axial tension force whose magnitude depends on the internal surface roughness within the pipeline is developed. This force offers a resistance to the vertical impact force (the pipe´s shell act as a membrane in tension) thereby reducing the indentation plastic energy absorbed and subsequently reducing the indentation depth.

On the other hand, there is little or no significant effect of the surrounding water on the response of the pipeline due to impact. It is however worth mentioning that the effect might be more pronounced at higher depths.

The DNV codes are well known for their high level of conservatism. As demonstrated in the comparisons above (7.4.6), the DNV values are on average 2.73 times higher than those obtained from the experimental based model.
When Statoil stepped up its design trawl board impact load by a factor of 2.9 (see 5.2), the overall level of conservatism increases to almost a factor of 8 i.e. 2.73 x 2.9.
As earlier mentioned above, some structures which were designed with designed requirement postulated by NORSOK U-001 and DNV RP-F111 have been reported to have collided with pretty much heavier trawl board(4400 kg) and acquired little or no significant damage from the interaction [22]. Is it really necessary for Statoil to step up the design impact load that high?

8.2 Recommendations for a full-scale impact test in water

The test performed above, was not scaled. This limitation and many others may have made the effect of the surrounding water unclear.

In order to reach a conclusive result, a full scale test is recommended. The test should also take into account the following:

- Investigation of the overall effect of water depth on the response of the pipeline. Model trails were performed at 100m depth, but most subsea structures are now found in much more higher depths

- The effect of damping due to surrounding water and its variation with depth.

- Quantize the effect variations in hydrodynamic added mass of the trawl board may have on the impact energy.

- Investigate the effect internal surface roughness may have on the impact resistance of the subsea structure, especially tubular shaped protective structures.

References

[1] Valdemarsen, J.W., Jørgensen, T. and Engås, A. (2007): Options to Mitigate Bottom Habitat Impact of Dragged Gears. FAO fisheries technical paper 506, Bergen, Norway

[2] Frits N. Jensen (2002): Description of Common Fishing Gear, Operational Procedures and Area of Operation. Barlindhaug Rådgivende ingeniører og økonomer.

[3] R.D Galbralth and A Rice (2004): An Introduction to Commercial Fishing Gear and Methods Used in Scotland. Scottish Fisheries Information Pamphlet No. 25. ISSN: 0309 9105

[4] http://en.wikipedia.org/wiki/Bottom_trawling#Body_of_the_trawl, visited on 25/03/2013

[5] DNV-RP-F111 (2010): Interference between Trawl Gear and Pipelines. Det Norske Veritas, Norway

[6] Valdemarsen, J.W., Jørgensen, T. and Engås, A. (2007): Options to Mitigate Bottom Habitat Impact of Dragged Gears. FAO fisheries technical paper 506, Bergen, Norway

[7] http://www.fao.org/fishery/geartype/305/en visisted on 07/04/2013

[8] http://www.ecomare.nl/en/ecomare-encyclopedie/man-and-the-environment/fisheries/fishery-techniques/beam-trawl-fisheries/ visited on 07/04/2013

[9] ISO 13628 - 1 (2005): Petroleum and natural gas industries -- Design and operation of subsea production systems -- Part 1: General requirements and recommendations

[11] Richard J. Charles (1954): Impact Studies on Fixed End Rods. Doctor of science research work at Massachusetts Institute of Technology, USA.

[12] http://blog.keytometals.com/true-stress-true-strain-curve-part-one-2/ visited on 29/04/2013

[13] Jones, N., R.S Birch, Low velocity impact of pressurised pipelines, International Journal of Impact Engineering, Vol. 37, 2010.

[14] Ellinas, C. P., Walker, A. C., Damage on offshore tubular bracing members. IABSE Colloquium on Ship Collisions with Bridges and Offshore Structures. Copenhagen, pp 253-261, 1983.

[15] De Oliveira, J. G., Wierzbicki, T., Abramowicz, W., Plastic behaviour of tubular members under lateral concentrated loading. Det Norske Veritas Tech. Rep. 82-0708, 1982.

[16] Jones, N., Birch, R. S., Influence of Internal Pressure on the Impact Behaviour of Steel Pipelines, Transactions ASME, Journal of Pressure Vessel Technology, Vol. 118, No. 4, 464-471, 1996.

[17] Jones, N., Shen, W. Q., A Theoretical Study of the Lateral Impact of Fully Clamped Pipelines, proceedings Institution of Mechanical Engineers, Vol. 206(E), pp 129-146, 1992.

[18] http://www.copper.org/applications/architecture/arch_dhb/fundamentals/intro.html , visited on 05/02/2013.

[19] Concept Development and Engineering (CD&E), Technical and professional requirement. TR1230 page 41 (2009)

[20] NORSOK standards U-001(2002) : Subsea Production Systems

[21] Pipeline/Trawl Gear Interaction. Shell´s design and engineering practise. Dep 31.40.10.17-Gen (April 2006).

[22] JIP- Møtereferat 09/11/2207, Det Norske Veritas

[23] HOST Protetction Structure-Overtrawling Tests (1996) . Konsberg Offshore AS

Appendix A:

A1. Velocity and Kinetic Energy of Striker

$U_o := 0\frac{m}{s}$ Inertia velocity of striker

$a := 9.81\frac{m}{s^2}$ Acceleration due to gravity

$S := 0.56m$ Distance travelled by striker

From Newton´s equation of motion

$$(V_o) := \left[(U_o)^2 + 2a \cdot S\right]^{\frac{1}{2}}$$

$V_o = 3.315\frac{m}{s}$

$G := 9.62kg, 11.02kg .. 15.22kg$ Masses of striker

The striker's kinetic energy is given by

$$E_{striker}(G) := \frac{1}{2} \cdot G \cdot V_o^{\,2}$$

$E_{striker}(G)$

52.848	J
60.539	
68.231	
75.922	
83.613	

A2. Maximum Strain

The Rankine´s criterion which states that ´´ Yielding begins at a point in a member where the maximum principal stress reaches a value equal to the tensile (or compressive) yield stress Y´´

This implies that at the yield point,

$\sigma = Y$ Where Y is the tensile yield strength

From the Hooke´s law

$$E_{xx} = \frac{\sigma_{xx} - \nu\left(\sigma_{yy} + \sigma_{zz}\right)}{Emod}$$

Where E_{mod} is the young´s modulus for the material

Assuming the following:
Pure elastic-plastic bending
Uniaxial stress

Then it follows that

$$\sigma_{xx} = Y$$

And

$$Ey = \frac{Y}{Emod} = E_{xx}$$

In case of the copper pipe

$$Emod := 120000MPa$$

$$Y := 310MPa$$

From

$$Ey := \frac{Y}{Emod}$$

$$Ey = 2.583 \times 10^{-3}$$

$$Ey = 0.00258$$

A3. ELASTIC STRAIN ENERGY

$D := 0.015m$ outer diameter

$t := 0.001m$ Wall thickness

$E := 1.2 \cdot 10^{11} \frac{N}{m^2}$

$A := \frac{\pi}{4} \cdot (D - 2 \cdot t)^2$

$A = 1.327 \times 10^{-4} m^2$

$\varepsilon := 2.583 \times 10^{-3}$ Maximum yield strain

$$W_s := \frac{A \cdot E}{2} \cdot \int_0^{0.032m} \varepsilon^2 \, dl$$

$W_s = 1.7J$

$$F_b = C_h \cdot V \cdot \left(m_a \cdot k_b\right)^{\frac{1}{2}}$$

A4. RECOMMENDED PRACTICE DNV-RP-F111

Trawl board impact energy

$m_t := 9.62kg, 11.02kg .. 15.22kg$

m_t

$C_h := 1$ Span height less than 0.3 m

$R_{fs} := 0.3778$ This value is got by extrapolation on fig 5.1.1-1

$V := 3.32 \frac{m}{s}$

$$E_s\left(m_t\right) := R_{fs} \cdot \frac{1}{2} \cdot m_t \cdot \left(C_h \cdot V\right)^2$$

$E_s\left(m_t\right) =$

20.03	J
22.945	
25.86	
28.775	
31.69	

Appendix B

B1. The Pipe´s Data

Material: Half Hard copper

$E := 117GPa$ Modulus of elasticity

$\sigma y := 207MPa$ (18) minimum yield strength

$\nu := 0.35$ Poisson´s ratio

$D := 15.04mm$ mean diameter of pipe

$R_0 := \frac{D}{2}$ mean radius of pipe

$R_0 = 7.52 \times 10^{-3} m$

$L_1 := \frac{300mm}{2}$ $L_1 = 0.15m$ Impact location of striker measured from a clamped support

$L := L_1$ $L = 0.15m$

$2L$ Length of fully clamped pipe

$H := 1.15mm$ Wall thickness of pipe

B2. Empty Pipe in Air

Element 1

$W_f := 3.28mm$

$D_m := 16.68mm$

$T_r := 11.73mm$

$$r_o := \frac{T_r}{2}\left[1 + \left(\frac{D_m}{2T_r}\right)^2\right]$$

$r_o = 8.83 \times 10^{-3} m$

$$\beta := \pi \frac{R_0}{2r_o}$$

$\beta = 1.338$

$$\cos\phi_o := \left(1 - \frac{T_r}{r_o}\right)$$

$$\delta := r_o\left(\cos(\beta) - \cos\phi_o\right)$$

$\delta = 4.939 \times 10^{-3} m$

$W_1 := (R_0 - \delta)$

$W_1 = 2.581 \times 10^{-3} m$

$W_g := (W_f - W_1)$

$W_g = 6.991 \times 10^{-4} m$

Ellinas and Walker

$K_o := 150$

$$\Delta\gamma := \frac{W_1}{2R_0}$$

$\Delta\gamma = 0.172$

$$W\gamma := \frac{W_g}{2R_0}$$

$W\gamma = 0.046$

Energy absorbed plastically during local indentation

$$Epl := \frac{R_0(K_o) H^2 \cdot (\sigma y)}{3} \Delta\gamma^{\frac{3}{2}}$$

$Epl = 7.317J$

Global plastic energy

$$E_{gl} := 16H \cdot (R_0)^3 \sigma y (1 + \cos(\beta) - \beta) \frac{W\gamma}{L}$$

$E_{gl} = -0.054J$

Oliveira , Wierzbicki and Abramowicz

$$k := 1 + \pi \cdot H \cdot \frac{\left(\frac{L}{R}\right)^2}{8R_0}$$

$$\Delta\gamma m := 2 \cdot \left[k - \left(k^2 - 1\right)^{\frac{1}{2}}\right]$$

Energy absorbed plastically during local indentation

$$E_{pl} := 8\pi^{\frac{1}{2}} \sigma y \frac{(H \cdot W_1)^{\frac{3}{2}}}{3}$$

$E_{pl} = 5.003J$

$$E_{glo} := \left[16\sigma y (R_0)^3 \frac{H}{L}\right]\left[\left(\frac{8}{\pi^2}\right)(1 - \Delta\gamma m)(2 - \Delta\gamma m) \sin\left[\pi^2 \frac{W\gamma}{8(1 - \Delta\gamma m)}\right] + \pi^2 \frac{W\gamma^3}{12(1 - \Delta\gamma m)}\right]$$

Energy absorbed during deformation-global

$E_{glo} = (0.984)J$

Element 2

$W_f := 3.21mm$

$D_m := 16.52mm$

$T_r := 11.80mm$

$$r_o := \frac{T_r}{2}\left[1 + \left(\frac{D_m}{2T_r}\right)^2\right]$$

$r_o = 8.791 \times 10^{-3} m$

$$\beta := \pi \frac{R_0}{2r_o}$$

$\beta = 1.344$

$$\cos\phi_o := \left(1 - \frac{T_r}{r_o}\right)$$

$\delta := r_o\left(\cos(\beta) - \cos\phi_o\right)$

$\delta = 4.988 \times 10^{-3} m$

$W_1 := (R_0 - \delta)$

$W_1 = 2.532 \times 10^{-3} m$

$W_g := (W_f - W_1)$

$W_g = 6.784 \times 10^{-4} m$

Ellinas and Walker

$K_o := 150$

$$\Delta\gamma := \frac{W_1}{2R_0}$$

$\Delta\gamma = 0.168$

$$W\gamma := \frac{W_g}{2R_0}$$

$W\gamma = 0.045$

$$Epl := \frac{R_0(K_o)H^2 \cdot (\sigma y)}{3}\Delta\gamma^{\frac{3}{2}}$$

Energy absorbed plastically during local indentation

$Epl = 7.109J$

Global plastic energy

$$E_{gl} := 16H \cdot (R_0)^3 \sigma y\left(1 + \cos(\beta) - \beta\right)\frac{W\gamma}{L}$$

$E_{gl} = -0.058J$

Oliveira , Wierzbicki and Abramowicz

$$k := 1 + \pi \cdot H \cdot \frac{\left(\frac{L}{R}\right)^2}{8R_0}$$

$$\Delta\gamma m := 2 \cdot \left[k - \left(k^2 - 1\right)^{\frac{1}{2}}\right]$$

Energy absorbed plastically during local indentation

$$E_{pl} := 8\pi^{\frac{1}{2}} \sigma y \frac{(H \cdot W_1)^{\frac{3}{2}}}{3}$$

$E_{pl} = 4.86J$

$$E_{glo} := \left[16\sigma y (R_0)^3 \frac{H}{L}\right]\left[\left(\frac{8}{\pi^2}\right)(1 - \Delta\gamma m)(2 - \Delta\gamma m)\sin\left[\pi^2 \frac{W\gamma}{8(1 - \Delta\gamma m)}\right] + \pi^2 \frac{W\gamma^3}{12(1 - \Delta\gamma m)}\right]$$

Energy absorbed during deformation-global

$E_{glo} = (0.955)J$

Element 3

$W_f := 3.42mm$

$D_m := 16.58mm$

$T_r := 11.59mm$

$$r_o := \frac{T_r}{2}\left[1 + \left(\frac{D_m}{2T_r}\right)^2\right]$$

$r_o = 8.76 \times 10^{-3} m$

$$\beta := \pi \frac{R_0}{2r_o}$$

$\beta = 1.348$

$$\cos\phi_o := \left(1 - \frac{T_r}{r_o}\right)$$

$\delta := r_o\left(\cos(\beta) - \cos\phi_o\right)$

$\delta = 4.762 \times 10^{-3} m$

$W_1 := (R_0 - \delta)$

$W_1 = 2.758 \times 10^{-3} m$

$W_g := (W_f - W_1)$

$W_g = 6.617 \times 10^{-4} m$

Ellinas and Walker

$K_o := 150$

$$\Delta\gamma := \frac{W_1}{2R_0}$$

$\Delta\gamma = 0.183$

$$W\gamma := \frac{W_g}{2R_0}$$

$W\gamma = 0.044$

Energy absorbed plastically during local indentation

$$Epl := \frac{R_0(K_o)H^2 \cdot (\sigma y)}{3}\Delta\gamma^{\frac{3}{2}}$$

$Epl = 8.084J$

Global plastic energy

$$E_{gl} := 16H \cdot (R_0)^3 \sigma y\left(1 + \cos(\beta) - \beta\right)\frac{W\gamma}{L}$$

$E_{gl} = -0.061J$

Oliveira , Wierzbicki and Abramowicz

$$k := 1 + \pi \cdot H \cdot \frac{\left(\frac{L}{R}\right)^2}{8R_0}$$

$$\Delta\gamma m := 2 \cdot \left[k - \left(k^2 - 1\right)^{\frac{1}{2}}\right]$$

Energy absorbed plastically during local indentation

$$E_{pl} := 8\pi^{\frac{1}{2}} \sigma y \frac{(H \cdot W_1)^{\frac{3}{2}}}{3}$$

$E_{pl} = 5.528J$

$$E_{glo} := \left[16\sigma y (R_0)^3 \frac{H}{L}\right]\left[\left(\frac{8}{\pi^2}\right)(1 - \Delta\gamma m)(2 - \Delta\gamma m)\sin\left[\pi^2 \frac{W\gamma}{8(1 - \Delta\gamma m)}\right] + \pi^2 \frac{W\gamma^3}{12(1 - \Delta\gamma m)}\right]$$

Energy absorbed during deformation-global

$E_{glo} = (0.931)J$

Element 4

$W_f := 3.50mm$

$D_m := 16.56mm$

$T_r := 11.51mm$

$$r_o := \frac{T_r}{2}\left[1 + \left(\frac{D_m}{2T_r}\right)^2\right]$$

$r_o = 8.733 \times 10^{-3} m$

$$\beta := \pi \frac{R_0}{2r_o}$$

$\beta = 1.353$

$$\cos\phi_o := \left(1 - \frac{T_r}{r_o}\right)$$

$\delta := r_o\left(\cos(\beta) - \cos\phi_o\right)$

$\delta = 4.667 \times 10^{-3} m$

$W_1 := (R_0 - \delta)$

$W_1 = 2.853 \times 10^{-3} m$

$W_g := (W_f - W_1)$

$W_g = 6.474 \times 10^{-4} m$

Ellinas and Walker

$K_o := 150$

$$\Delta\gamma := \frac{W_1}{2R_0}$$

$\Delta\gamma = 0.19$

$$W\gamma := \frac{W_g}{2R_0}$$

$W\gamma = 0.043$

Energy absorbed plastically during local indentation

$$Epl := \frac{R_0(K_o)H^2 \cdot (\sigma y)}{3}\Delta\gamma^{\frac{3}{2}}$$

$Epl = 8.502J$

Global plastic energy

$$E_{gl} := 16H \cdot (R_0)^3 \sigma y\left(1 + \cos(\beta) - \beta\right)\frac{W\gamma}{L}$$

$E_{gl} = -0.063J$

Oliveira , Wierzbicki and Abramowicz

$$k := 1 + \pi \cdot H \cdot \frac{\left(\frac{L}{R}\right)^2}{8R_0}$$

$$\Delta\gamma m := 2 \cdot \left[k - \left(k^2 - 1\right)^{\frac{1}{2}}\right]$$

Energy absorbed plastically during local indentation

$$E_{pl} := 8\pi^{\frac{1}{2}} \sigma y \frac{(H \cdot W_1)^{\frac{3}{2}}}{3}$$

$E_{pl} = 5.813J$

$$E_{glo} := \left[16\sigma y (R_0)^3 \frac{H}{L}\right]\left[\left(\frac{8}{\pi^2}\right)(1 - \Delta\gamma m)(2 - \Delta\gamma m)\sin\left[\pi^2 \frac{W\gamma}{8(1 - \Delta\gamma m)}\right] + \pi^2 \frac{W\gamma^3}{12(1 - \Delta\gamma m)}\right]$$

Energy absorbed during deformation-global

$E_{glo} = (0.911)J$

Element 5

$W_f := 3.56mm$

$D_m := 16.46mm$

$T_r := 11.45mm$

$$r_o := \frac{T_r}{2}\left[1 + \left(\frac{D_m}{2T_r}\right)^2\right]$$

$r_o = 8.683 \times 10^{-3}\,m$

$$\beta := \pi\frac{R_0}{2r_o}$$

$\beta = 1.36$

$$\cos\phi_o := \left(1 - \frac{T_r}{r_o}\right)$$

$\delta := r_o\left(\cos(\beta) - \cos\phi_o\right)$

$\delta = 4.58 \times 10^{-3}\,m$

$W_1 := (R_0 - \delta)$

$W_1 = 2.94 \times 10^{-3}\,m$

$W_g := (W_f - W_1)$

$W_g = 6.203 \times 10^{-4}\,m$

Ellinas and Walker

$K_o := 150$

$$\Delta\gamma := \frac{W_1}{2R_0}$$

$\Delta\gamma = 0.195$

$$W\gamma := \frac{W_g}{2R_0}$$

$W\gamma = 0.041$

Energy absorbed plastically during local indentation

$$Epl := \frac{R_0(K_o)H^2\cdot(\sigma y)}{3}\Delta\gamma^{\frac{3}{2}}$$

$Epl = 8.895J$

Global plastic energy

$$E_{gl} := 16H\cdot(R_0)^3\sigma y(1 + \cos(\beta) - \beta)\frac{W\gamma}{L}$$

$E_{gl} = -0.068J$

Oliveira , Wierzbicki and Abramowicz

$$k := 1 + \pi\cdot H\cdot\frac{\left(\frac{L}{R}\right)^2}{8R_0}$$

$$\Delta\gamma m := 2\cdot\left[k - \left(k^2 - 1\right)^{\frac{1}{2}}\right]$$

Energy absorbed plastically during local indentation

$$E_{pl} := 8\pi^{\frac{1}{2}}\sigma y\frac{(H\cdot W_1)^{\frac{3}{2}}}{3}$$

$E_{pl} = 6.082J$

$$E_{glo} := \left[16\sigma y(R_0)^3\frac{H}{L}\right]\left[\left(\frac{8}{\pi^2}\right)(1 - \Delta\gamma m)(2 - \Delta\gamma m)\sin\left[\pi^2\frac{W\gamma}{8(1 - \Delta\gamma m)}\right] + \pi^2\frac{W\gamma^3}{12(1 - \Delta\gamma m)}\right]$$

Energy absorbed during deformation-global

$E_{glo} = (0.873)\,J$

B3. Water-Filled Pipes in Air

Element 1

$W_f := 3.09mm$

$D_m := 16.53mm$

$T_r := 11.92mm$

$$r_o := \frac{T_r}{2}\left[1 + \left(\frac{D_m}{2T_r}\right)^2\right]$$

$r_o = 8.825 \times 10^{-3} m$

$$\beta := \pi \frac{R_0}{2r_o}$$

$\beta = 1.338$

$$\cos\phi_o := \left(1 - \frac{T_r}{r_o}\right)$$

$\delta := r_o\left(\cos(\beta) - \cos\phi_o\right)$

$\delta = 5.127 \times 10^{-3} m$

$W_1 := (R_0 - \delta)$

$W_1 = 2.393 \times 10^{-3} m$

$W_g := (W_f - W_1)$

$W_g = 6.967 \times 10^{-4} m$

Ellinas and Walker

$K_o := 150$

$$\Delta\gamma := \frac{W_1}{2R_0}$$

$\Delta\gamma = 0.159$

$$W\gamma := \frac{W_g}{2R_0}$$

$W\gamma = 0.046$

Energy absorbed plastically during local indentation

$$Epl := \frac{R_0(K_o)H^2 \cdot (\sigma y)}{3}\Delta\gamma^{\frac{3}{2}}$$

$Epl = 6.534J$

Global plastic energy

$$E_{gl} := 16H \cdot (R_0)^3 \sigma y\left(1 + \cos(\beta) - \beta\right)\frac{W\gamma}{L}$$

$E_{gl} = -0.054J$

Oliveira , Wierzbicki and Abramowicz

$$k := 1 + \pi \cdot H \cdot \frac{\left(\frac{L}{R}\right)^2}{8R_0}$$

$$\Delta\gamma m := 2 \cdot \left[k - \left(k^2 - 1\right)^{\frac{1}{2}}\right]$$

Energy absorbed plastically during local indentation

$$E_{pl} := 8\pi^{\frac{1}{2}} \sigma y \frac{(H \cdot W_1)^{\frac{3}{2}}}{3}$$

$E_{pl} = 4.467J$

$$E_{glo} := \left[16\sigma y (R_0)^3 \frac{H}{L}\right]\left[\left(\frac{8}{\pi^2}\right)(1 - \Delta\gamma m)(2 - \Delta\gamma m)\sin\left[\pi^2 \frac{W\gamma}{8(1 - \Delta\gamma m)}\right] + \pi^2 \frac{W\gamma^3}{12(1 - \Delta\gamma m)}\right]$$

Energy absorbed during deformation-global

$E_{glo} = (0.981)J$

Element 2

$W_f := 3.19mm$

$D_m := 16.52mm$

$T_r := 11.82mm$

$$r_o := \frac{T_r}{2}\left[1 + \left(\frac{D_m}{2T_r}\right)^2\right]$$

$r_o = 8.796 \times 10^{-3} m$

$$\beta := \pi \frac{R_0}{2r_o}$$

$\beta = 1.343$

$$\cos\phi_o := \left(1 - \frac{T_r}{r_o}\right)$$

$\delta := r_o\left(\cos(\beta) - \cos\phi_o\right)$

$\delta = 5.011 \times 10^{-3} m$

$W_1 := (R_0 - \delta)$

$W_1 = 2.509 \times 10^{-3} m$

$W_g := (W_f - W_1)$

$W_g = 6.811 \times 10^{-4} m$

Ellinas and Walker

$K_o := 150$

$$\Delta\gamma := \frac{W_1}{2R_0}$$

$\Delta\gamma = 0.167$

$$W\gamma := \frac{W_g}{2R_0}$$

$W\gamma = 0.045$

Energy absorbed plastically during local indentation

$$Epl := \frac{R_0(K_o)H^2 \cdot (\sigma y)}{3}\Delta\gamma^{\frac{3}{2}}$$

$Epl = 7.013J$

Global plastic energy

$$E_{gl} := 16H \cdot (R_0)^3 \sigma y(1 + \cos(\beta) - \beta)\frac{W\gamma}{L}$$

$E_{gl} = -0.057J$

Oliveira , Wierzbicki and Abramowicz

$$k := 1 + \pi \cdot H \cdot \frac{\left(\frac{L}{R}\right)^2}{8R_0}$$

$$\Delta\gamma m := 2 \cdot \left[k - \left(k^2 - 1\right)^{\frac{1}{2}}\right]$$

Energy absorbed plastically during local indentation

$$E_{pl} := 8\pi^{\frac{1}{2}} \sigma y \frac{(H \cdot W_1)^{\frac{3}{2}}}{3}$$

$E_{pl} = 4.795J$

$$E_{glo} := \left[16\sigma y(R_0)^3 \frac{H}{L}\right]\left[\left(\frac{8}{\pi^2}\right)(1 - \Delta\gamma m)(2 - \Delta\gamma m)\sin\left[\pi^2 \frac{W\gamma}{8(1 - \Delta\gamma m)}\right] + \pi^2 \frac{W\gamma^3}{12(1 - \Delta\gamma m)}\right]$$

Energy absorbed during deformation-global

$E_{glo} = (0.959)J$

Element 3

$W_f := 3.31mm$

$D_m := 16.63mm$

$T_r := 11.70mm$

$$r_o := \frac{T_r}{2}\left[1 + \left(\frac{D_m}{2T_r}\right)^2\right]$$

$r_o = 8.805 \times 10^{-3} m$

$$\beta := \pi \frac{R_0}{2r_o}$$

$\beta = 1.342$

$$\cos\phi_o := \left(1 - \frac{T_r}{r_o}\right)$$

$\delta := r_o\left(\cos(\beta) - \cos\phi_o\right)$

$\delta = 4.896 \times 10^{-3} m$

$W_1 := (R_0 - \delta)$

$W_1 = 2.624 \times 10^{-3} m$

$W_g := (W_f - W_1)$

$W_g = 6.857 \times 10^{-4} m$

Ellinas and Walker

$K_o := 150$

$$\Delta\gamma := \frac{W_1}{2R_0}$$

$\Delta\gamma = 0.174$

$$W\gamma := \frac{W_g}{2R_0}$$

$W\gamma = 0.046$

Energy absorbed plastically during local indentation

$$Epl := \frac{R_0(K_o) H^2 \cdot (\sigma y)}{3} \Delta\gamma^{\frac{3}{2}}$$

$Epl = 7.503J$

Global plastic energy

$$E_{gl} := 16H \cdot (R_0)^3 \sigma y (1 + \cos(\beta) - \beta) \frac{W\gamma}{L}$$

$E_{gl} = -0.056J$

Oliveira , Wierzbicki and Abramowicz

$$k := 1 + \pi \cdot H \cdot \frac{\left(\frac{L}{R}\right)^2}{8R_0}$$

$$\Delta\gamma m := 2 \cdot \left[k - \left(k^2 - 1\right)^{\frac{1}{2}}\right]$$

Energy absorbed plastically during local indentation

$$E_{pl} := 8\pi^{\frac{1}{2}} \sigma y \frac{(H \cdot W_1)^{\frac{3}{2}}}{3}$$

$E_{pl} = 5.13J$

$$E_{glo} := \left[16\sigma y (R_0)^3 \frac{H}{L}\right]\left[\left(\frac{8}{\pi^2}\right)(1 - \Delta\gamma m)(2 - \Delta\gamma m) \sin\left[\pi^2 \frac{W\gamma}{8(1 - \Delta\gamma m)}\right] + \pi^2 \frac{W\gamma^3}{12(1 - \Delta\gamma m)}\right]$$

Energy absorbed during deformation-global

$E_{glo} = (0.965) J$

Element 4

$W_f := 3.43mm$

$D_m := 16.64mm$

$T_r := 11.58mm$

$$r_o := \frac{T_r}{2}\left[1 + \left(\frac{D_m}{2T_r}\right)^2\right]$$

$r_o = 8.779 \times 10^{-3} m$

$$\beta := \pi \frac{R_0}{2r_o}$$

$\beta = 1.346$

$$\cos\phi_o := \left(1 - \frac{T_r}{r_o}\right)$$

$\delta := r_o\left(\cos(\beta) - \cos\phi_o\right)$

$\delta = 4.762 \times 10^{-3} m$

$W_1 := \left(R_0 - \delta\right)$

$W_1 = 2.758 \times 10^{-3} m$

$W_g := \left(W_f - W_1\right)$

$W_g = 6.719 \times 10^{-4} m$

Ellinas and Walker

$K_o := 150$

$$\Delta\gamma := \frac{W_1}{2R_0}$$

$\Delta\gamma = 0.183$

$$W\gamma := \frac{W_g}{2R_0}$$

$W\gamma = 0.045$

Energy absorbed plastically during local indentation

$$Epl := \frac{R_0\left(K_o\right) H^2 \cdot (\sigma y)}{3} \Delta\gamma^{\frac{3}{2}}$$

$Epl = 8.084J$

Global plastic energy

$$E_{gl} := 16H \cdot \left(R_0\right)^3 \sigma y \left(1 + \cos(\beta) - \beta\right) \frac{W\gamma}{L}$$

$E_{gl} = -0.059J$

Oliveira , Wierzbicki and Abramowicz

$$k := 1 + \pi \cdot H \cdot \frac{\left(\frac{L}{R}\right)^2}{8R_0}$$

$$\Delta\gamma m := 2 \cdot \left[k - \left(k^2 - 1\right)^{\frac{1}{2}}\right]$$

Energy absorbed plastically during local indentation

$$E_{pl} := 8\pi^{\frac{1}{2}} \sigma y \frac{\left(H \cdot W_1\right)^{\frac{3}{2}}}{3}$$

$E_{pl} = 5.527J$

$$E_{glo} := \left[16\sigma y \left(R_0\right)^3 \frac{H}{L}\right]\left[\left(\frac{8}{\pi^2}\right)(1 - \Delta\gamma m)(2 - \Delta\gamma m) \sin\left[\pi^2 \frac{W\gamma}{8(1 - \Delta\gamma m)}\right] + \pi^2 \frac{W\gamma^3}{12(1 - \Delta\gamma m)}\right]$$

Energy absorbed during deformation-global

$E_{glo} = (0.946)\,J$

Element 5

$W_f := 3.47mm$

$D_m := 16.71mm$

$T_r := 11.54mm$

$$r_o := \frac{T_r}{2}\left[1 + \left(\frac{D_m}{2T_r}\right)^2\right]$$

$r_o = 8.795 \times 10^{-3} m$

$$\beta := \pi \frac{R_0}{2r_o}$$

$\beta = 1.343$

$$\cos\phi_o := \left(1 - \frac{T_r}{r_o}\right)$$

$\delta := r_o\left(\cos(\beta) - \cos\phi_o\right)$

$\delta = 4.73 \times 10^{-3} m$

$W_1 := (R_0 - \delta)$

$W_1 = 2.79 \times 10^{-3} m$

$W_g := (W_f - W_1)$

$W_g = 6.802 \times 10^{-4} m$

Ellinas and Walker

$K_o := 150$

$$\Delta\gamma := \frac{W_1}{2R_0}$$

$\Delta\gamma = 0.185$

$$W\gamma := \frac{W_g}{2R_0}$$

$W\gamma = 0.045$

Energy absorbed plastically during local indentation

$$Epl := \frac{R_0(K_o)H^2 \cdot (\sigma y)}{3}\Delta\gamma^{\frac{3}{2}}$$

$Epl = 8.223J$

Global plastic energy

$$E_{gl} := 16H \cdot (R_0)^3 \sigma y\left(1 + \cos(\beta) - \beta\right)\frac{W\gamma}{L}$$

$E_{gl} = -0.057J$

Oliveira , Wierzbicki and Abramowicz

$$k := 1 + \pi \cdot H \cdot \frac{\left(\frac{L}{R}\right)^2}{8R_0}$$

$$\Delta\gamma m := 2 \cdot \left[k - \left(k^2 - 1\right)^{\frac{1}{2}}\right]$$

Energy absorbed plastically during local indentation

$$E_{pl} := 8\pi^{\frac{1}{2}} \sigma y \frac{(H \cdot W_1)^{\frac{3}{2}}}{3}$$

$E_{pl} = 5.622J$

$$E_{glo} := \left[16\sigma y (R_0)^3 \frac{H}{L}\right]\left[\left(\frac{8}{\pi^2}\right)(1 - \Delta\gamma m)(2 - \Delta\gamma m)\sin\left[\pi^2 \frac{W\gamma}{8(1 - \Delta\gamma m)}\right] + \pi^2 \frac{W\gamma^3}{12(1 - \Delta\gamma m)}\right]$$

Energy absorbed during deformation-global

$E_{glo} = (0.957)J$

B4. Water-Filled Pipes in Water

Element 1

$W_f := 3.07mm$

$D_m := 16.48mm$

$T_r := 11.94mm$

$$r_o := \frac{T_r}{2}\left[1 + \left(\frac{D_m}{2T_r}\right)^2\right]$$

$r_o = 8.813 \times 10^{-3} m$

$$\beta := \pi \frac{R_0}{2r_o}$$

$\beta = 1.34$

$$\cos\phi_o := \left(1 - \frac{T_r}{r_o}\right)$$

$\delta := r_o\left(\cos(\beta) - \cos\phi_o\right)$

$\delta = 5.14 \times 10^{-3} m$

$W_1 := (R_0 - \delta)$

$W_1 = 2.38 \times 10^{-3} m$

$W_g := (W_f - W_1)$

$W_g = 6.903 \times 10^{-4} m$

Ellinas and Walker

$K_o := 150$

$$\Delta\gamma := \frac{W_1}{2R_0}$$

$\Delta\gamma = 0.158$

$$W\gamma := \frac{W_g}{2R_0}$$

$W\gamma = 0.046$

Energy absorbed plastically during local indentation

$$Epl := \frac{R_0(K_o)H^2 \cdot (\sigma y)}{3}\Delta\gamma^{\frac{3}{2}}$$

$Epl = 6.479J$

Global plastic energy

$$E_{gl} := 16H \cdot (R_0)^3 \sigma y\left(1 + \cos(\beta) - \beta\right)\frac{W\gamma}{L}$$

$E_{gl} = -0.055J$

Oliveira , Wierzbicki and Abramowicz

$$k := 1 + \pi \cdot H \cdot \frac{\left(\frac{L}{R}\right)^2}{8R_0}$$

$$\Delta\gamma m := 2 \cdot \left[k - \left(k^2 - 1\right)^{\frac{1}{2}}\right]$$

Energy absorbed plastically during local indentation

$$E_{pl} := 8\pi^{\frac{1}{2}} \sigma y \frac{(H \cdot W_1)^{\frac{3}{2}}}{3}$$

$E_{pl} = 4.43J$

$$E_{glo} := \left[16\sigma y (R_0)^3 \frac{H}{L}\right]\left[\left(\frac{8}{\pi^2}\right)(1 - \Delta\gamma m)(2 - \Delta\gamma m)\sin\left[\pi^2 \frac{W\gamma}{8(1 - \Delta\gamma m)}\right] + \pi^2 \frac{W\gamma^3}{12(1 - \Delta\gamma m)}\right]$$

Energy absorbed during deformation-global

$E_{glo} = (0.972)J$

Element 2

$W_f := 3.18mm$

$D_m := 16.53mm$

$T_r := 11.83mm$

$$r_o := \frac{T_r}{2}\left[1 + \left(\frac{D_m}{2T_r}\right)^2\right]$$

$r_o = 8.802 \times 10^{-3} m$

$$\beta := \pi \frac{R_0}{2r_o}$$

$\beta = 1.342$

$$\cos\phi_o := \left(1 - \frac{T_r}{r_o}\right)$$

$\delta := r_o\left(\cos(\beta) - \cos\phi_o\right)$

$\delta = 5.024 \times 10^{-3} m$

$W_1 := (R_0 - \delta)$

$W_1 = 2.496 \times 10^{-3} m$

$W_g := (W_f - W_1)$

$W_g = 6.843 \times 10^{-4} m$

Ellinas and Walker

$K_o := 150$

$$\Delta\gamma := \frac{W_1}{2R_0}$$

$\Delta\gamma = 0.166$

$$W\gamma := \frac{W_g}{2R_0}$$

$W\gamma = 0.046$

Energy absorbed plastically during local indentation

$$Epl := \frac{R_0(K_o)H^2 \cdot (\sigma y)}{3}\Delta\gamma^{\frac{3}{2}}$$

$Epl = 6.958J$

Global plastic energy

$$E_{gl} := 16H \cdot (R_0)^3 \sigma y\left(1 + \cos(\beta) - \beta\right)\frac{W\gamma}{L}$$

$E_{gl} = -0.057J$

Oliveira , Wierzbicki and Abramowicz

$$k := 1 + \pi \cdot H \cdot \frac{\left(\frac{L}{R}\right)^2}{8R_0}$$

$$\Delta\gamma m := 2 \cdot \left[k - \left(k^2 - 1\right)^{\frac{1}{2}}\right]$$

Energy absorbed plastically during local indentation

$$E_{pl} := 8\pi^{\frac{1}{2}} \sigma y \frac{(H \cdot W_1)^{\frac{3}{2}}}{3}$$

$E_{pl} = 4.757J$

$$E_{glo} := \left[16\sigma y (R_0)^3 \frac{H}{L}\right]\left[\left(\frac{8}{\pi^2}\right)(1 - \Delta\gamma m)(2 - \Delta\gamma m)\sin\left[\pi^2 \frac{W\gamma}{8(1 - \Delta\gamma m)}\right] + \pi^2 \frac{W\gamma^3}{12(1 - \Delta\gamma m)}\right]$$

Energy absorbed during deformation-global

$E_{glo} = (0.963)J$

Element 3

$W_f := 3.39mm$

$D_m := 16.62mm$

$T_r := 11.62mm$

$$r_o := \frac{T_r}{2}\left[1 + \left(\frac{D_m}{2T_r}\right)^2\right]$$

$r_o = 8.781 \times 10^{-3} m$

$$\beta := \pi \frac{R_0}{2r_o}$$

$\beta = 1.345$

$$\cos\phi_o := \left(1 - \frac{T_r}{r_o}\right)$$

$\delta := r_o\left(\cos(\beta) - \cos\phi_o\right)$

$\delta = 4.803 \times 10^{-3} m$

$W_1 := (R_0 - \delta)$

$W_1 = 2.717 \times 10^{-3} m$

$W_g := (W_f - W_1)$

$W_g = 6.733 \times 10^{-4} m$

Ellinas and Walker

$K_o := 150$

$$\Delta\gamma := \frac{W_1}{2R_0}$$

$\Delta\gamma = 0.181$

$$W\gamma := \frac{W_g}{2R_0}$$

$W\gamma = 0.045$

Energy absorbed plastically during local indentation

$$Epl := \frac{R_0(K_o)H^2 \cdot (\sigma y)}{3}\Delta\gamma^{\frac{3}{2}}$$

$Epl = 7.902J$

Global plastic energy

$$E_{gl} := 16H \cdot (R_0)^3 \sigma y\left(1 + \cos(\beta) - \beta\right)\frac{W\gamma}{L}$$

$E_{gl} = -0.059J$

Oliveira , Wierzbicki and Abramowicz

$$k := 1 + \pi \cdot H \cdot \frac{\left(\frac{L}{R}\right)^2}{8R_0}$$

$$\Delta\gamma m := 2 \cdot \left[k - \left(k^2 - 1\right)^{\frac{1}{2}}\right]$$

Energy absorbed plastically during local indentation

$$E_{pl} := 8\pi^{\frac{1}{2}} \sigma y \frac{(H \cdot W_1)^{\frac{3}{2}}}{3}$$

$E_{pl} = 5.403J$

$$E_{glo} := \left[16\sigma y (R_0)^3 \frac{H}{L}\right]\left[\left(\frac{8}{\pi^2}\right)(1 - \Delta\gamma m)(2 - \Delta\gamma m)\sin\left[\pi^2 \frac{W\gamma}{8(1 - \Delta\gamma m)}\right] + \pi^2 \frac{W\gamma^3}{12(1 - \Delta\gamma m)}\right]$$

Energy absorbed during deformation-global

$E_{glo} = (0.948)J$

Element 4

$W_f := 3.44mm$

$D_m := 16.60mm$

$T_r := 11.57mm$

$$r_o := \frac{T_r}{2}\left[1 + \left(\frac{D_m}{2T_r}\right)^2\right]$$

$r_o = 8.762 \times 10^{-3} m$

$$\beta := \pi \frac{R_0}{2r_o}$$

$\beta = 1.348$

$$\cos\phi_o := \left(1 - \frac{T_r}{r_o}\right)$$

$\delta := r_o\left(\cos(\beta) - \cos\phi_o\right)$

$\delta = 4.743 \times 10^{-3} m$

$W_1 := (R_0 - \delta)$

$W_1 = 2.777 \times 10^{-3} m$

$W_g := (W_f - W_1)$

$W_g = 6.629 \times 10^{-4} m$

Ellinas and Walker

$K_o := 150$

$$\Delta\gamma := \frac{W_1}{2R_0}$$

$\Delta\gamma = 0.185$

$$W\gamma := \frac{W_g}{2R_0}$$

$W\gamma = 0.044$

Energy absorbed plastically during local indentation

$$Epl := \frac{R_0(K_o)H^2 \cdot (\sigma y)}{3}\Delta\gamma^{\frac{3}{2}}$$

$Epl = 8.167J$

Global plastic energy

$$E_{gl} := 16H \cdot (R_0)^3 \sigma y\left(1 + \cos(\beta) - \beta\right)\frac{W\gamma}{L}$$

$E_{gl} = -0.061J$

Oliveira , Wierzbicki and Abramowicz

$$k := 1 + \pi \cdot H \cdot \frac{\left(\frac{L}{R}\right)^2}{8R_0}$$

$$\Delta\gamma m := 2 \cdot \left[k - \left(k^2 - 1\right)^{\frac{1}{2}}\right]$$

Energy absorbed plastically during local indentation

$$E_{pl} := 8\pi^{\frac{1}{2}} \sigma y \frac{(H \cdot W_1)^{\frac{3}{2}}}{3}$$

$E_{pl} = 5.584J$

$$E_{glo} := \left[16\sigma y (R_0)^3 \frac{H}{L}\right]\left[\left(\frac{8}{\pi^2}\right)(1 - \Delta\gamma m)(2 - \Delta\gamma m)\sin\left[\pi^2 \frac{W\gamma}{8(1 - \Delta\gamma m)}\right] + \pi^2 \frac{W\gamma^3}{12(1 - \Delta\gamma m)}\right]$$

Energy absorbed during deformation-global

$E_{glo} = (0.933)J$

Element 5

$W_f := 3.54mm$

$D_m := 16.70mm$

$T_r := 11.47mm$

$$r_o := \frac{T_r}{2}\left[1 + \left(\frac{D_m}{2T_r}\right)^2\right]$$

$r_o = 8.774 \times 10^{-3} m$

$$\beta := \pi \frac{R_0}{2r_o}$$

$\beta = 1.346$

$$\cos\phi_o := \left(1 - \frac{T_r}{r_o}\right)$$

$\delta := r_o\left(\cos(\beta) - \cos\phi_o\right)$

$\delta = 4.649 \times 10^{-3} m$

$W_1 := (R_0 - \delta)$

$W_1 = 2.871 \times 10^{-3} m$

$W_g := (W_f - W_1)$

$W_g = 6.695 \times 10^{-4} m$

Ellinas and Walker

$K_o := 150$

$$\Delta\gamma := \frac{W_1}{2R_0}$$

$\Delta\gamma = 0.191$

$$W\gamma := \frac{W_g}{2R_0}$$

$W\gamma = 0.045$

Energy absorbed plastically during local indentation

$$Epl := \frac{R_0(K_o)H^2 \cdot (\sigma y)}{3}\Delta\gamma^{\frac{3}{2}}$$

$Epl = 8.583J$

Global plastic energy

$$E_{gl} := 16H \cdot (R_0)^3 \sigma y\left(1 + \cos(\beta) - \beta\right)\frac{W\gamma}{L}$$

$E_{gl} = -0.059J$

Oliveira , Wierzbicki and Abramowicz

$$k := 1 + \pi \cdot H \cdot \frac{\left(\frac{L}{R}\right)^2}{8R_0}$$

$$\Delta\gamma m := 2 \cdot \left[k - \left(k^2 - 1\right)^{\frac{1}{2}}\right]$$

Energy absorbed plastically during local indentation

$$E_{pl} := 8\pi^{\frac{1}{2}} \sigma y \frac{(H \cdot W_1)^{\frac{3}{2}}}{3}$$

$E_{pl} = 5.868J$

$$E_{glo} := \left[16\sigma y (R_0)^3 \frac{H}{L}\right]\left[\left(\frac{8}{\pi^2}\right)(1 - \Delta\gamma m)(2 - \Delta\gamma m)\sin\left[\pi^2 \frac{W\gamma}{8(1 - \Delta\gamma m)}\right] + \pi^2 \frac{W\gamma^3}{12(1 - \Delta\gamma m)}\right]$$

Energy absorbed during deformation-global

$E_{glo} = (0.942)J$